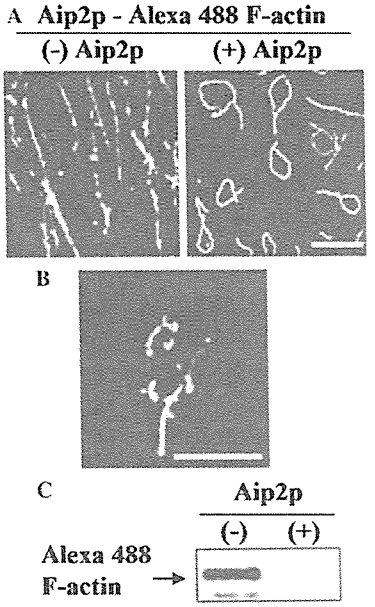

Fig. 1. (A) Formation of circular F-actin in vitro. Alexa 488-conjugated actin (Molecular Probes) was polymerized in high salt buffer (10 mM Tris–Cl (pH 8.0), 100 mM KCl, and 2 mM $MgCl_2$) and incubated with or without Aip2p in the presence of 1 mM ATP. Scale bar is 5 μm. (B) Anti-Aip2p antibody stains the circular F-actin in a discontinuous pattern. Alexa 594-conjugated anti-Aip2p antibody (red) was incubated with Alexa 488-conjugated F-actin (green) as described in Materials and methods. Samples were examined by fluorescent microscopy. Scale bar is 5 μm. (C) Trypsin susceptibility of Aip2p-bound circular F-actin is increased. Alexa 488-conjugated F-actin was incubated with Aip2p and ATP as described in Materials and methods. Samples were examined by fluorescent microscopy and subjected to the trypsin susceptibility assay.

radius of the circular F-actin was approximately 2–4 μm, which remained constant under the reaction conditions used in this study (Aip2p:F-actin = 1:1–1:5) (data not shown). The circularization process was very efficient as over 60% of the F-actin changed into circular form after incubation with Aip2p at 30 °C for 30 min. Alexa 488-conjugated anti-Aip2p antibody stained the circular F-actin in a discontinuous pattern (Fig. 1B). Incubation of Alexa 488-conjugated F-actin with Aip2p did not increase the rate of G-actin (see Fig. 1A). Alexa 488-conjugated F-actin was incubated with or without Aip2p as described above, treated with trypsin, and then subjected to Western blot analysis. The protease susceptibility of the Aip2p-bound "circular form" of F-actin clearly increased (Fig. 1C), indicating that the Aip2p-bound "circular form" of F-actin possesses an aberrant conformation compared to the linear form of F-actin.

Altered yeast cell morphology after the AIP2 modification

The phenotypic abnormalities were observed following modification of AIP2 expression. When Aip2p was overexpressed in yeast cells using the multicopy expression vector pYES2 and cultured under Aip2p-inducible conditions, cells produced multi-buds from the same mother neck or exhibited elongated bud necks (Fig. 2A, Overexpressed). This suggested that an excessive amount of Aip2p resulted in an abnormal budding process in yeast cells. In contrast, AIP2-deleted cells displayed deformed morphology reflecting an inability to properly form the cleavage furrow during cell division (Fig. 2A, Disrupted). The expression of intact Aip2p in the AIP2-deleted cells rescued this morphological defect (Fig. 2A, Plasmid rescue (AIP2)).

Because an abnormal actin cytoskeleton is considered as a major cause of such altered yeast cell morphology [15], the distribution of F-actin was examined in wild-type yeast cells, AIP2-deleted cells, and AIP2-overexpressed cells using rhodamine–phalloidin staining, which specifically stains F-actin in yeast cells. F-actin

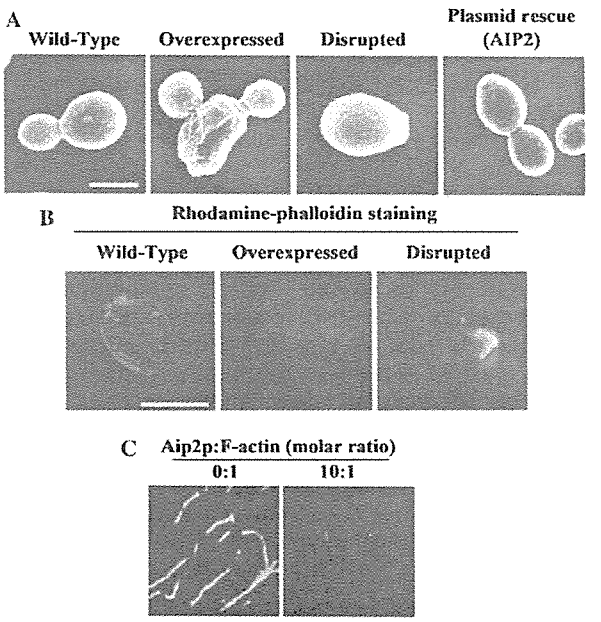

Fig. 2. (A) Wild-type (Wild-Type), AIP2-overexpressed (Overexpressed), and AIP2-deleted (Disrupted) strains were visualized using scanning electron microscopy (SEM). AIP2-overexpressed yeast cells produced multi-buds, while AIP2-deleted cells could not generate a proper cleavage furrow. The expression of AIP2 restored the cell morphology defect of the deleted strain (Plasmid rescue, AIP2). The AIP2-deleted strain was transformed with the pAUR123 plasmid carrying the gene for Aip2p under control of the ADH promoter. All transformants were cultured to an OD of 0.5–0.8 at 600 nm and then observed with SEM. Scale bar is 2 μm. (B) F-actin distribution with or without Aip2p in vivo. Wild-type yeast (Wild-Type), AIP2-deleted cells (Disrupted), and AIP2-overexpressed cells (Overexpressed) were incubated with 6.6 μM of rhodamine–phalloidin (red). Yeast cell wall was counterstained by Calcofluor White (Sigma) shown as blue. (C) F-actin distribution with or without Aip2p in vitro. Rabbit muscle actin (Molecular Probes) was polymerized, incubated with (10:1) or without (0:1) Aip2p in the presence of 1 mM ATP, and then stained with 6.6 μM of rhodamine–phalloidin.

was found to be clustered in the AIP2-deleted cells (Fig. 2B, right panel, Disrupted) compared to wild-type cells (Fig. 2B, left panel, Wild-Type). In contrast, when Aip2p was overexpressed in the wild-type strain using a multicopy expression vector, rhodamine–phalloidin-stained F-actin was only sparsely observed (Fig. 2B, middle panel, Overexpressed).

The in vitro rhodamine–phalloidin staining profile of F-actin on a glass slide varied considerably from that of F-actin incubated with Aip2p. Rhodamine–phalloidin hardly detected F-actin following incubation with Aip2p (Fig. 2C, right panel, 10:1) compared to the rhodamine–phalloidin staining profile of F-actin in the absence of Aip2p (Fig. 2C, left panel, 0:1). When fluorescently labeled G-actin was polymerized and used as a substrate (Alexa 488-conjugated F-actin), on the other hand, the fluorescent signals were not altered even after the incubation with Aip2p (see Fig. 1A). The total F-/G-actin contents remained at the same level after the AIP2-modification (data not shown).

Taken together, the incubation with Aip2p either competitively interferes with the rhodamine–phalloidin staining of F-actin or modifies the conformation of F-actin which the rhodamine–phalloidin hardly stained. The fact that the in vitro formation of circular F-actin (Fig. 1A) with its modified trypsin susceptibility (Fig. 1C) after the incubation with Aip2p supports the latter notion. Furthermore, the AIP2-deleted cells became sensitive to osmotic conditions (Fig. 3A), which is a hallmark of actin dysfunction [15]. Finally, immunoprecipitation of yeast cells using anti-Aip2p antibody demonstrated that Aip2p associates with actin (Fig. 3B, left panel). The reciprocal immunoprecipitation experiment using anti-actin antibody showed that Aip2p is contained in a complex with anti-actin antibody (Fig. 3B, right panel).

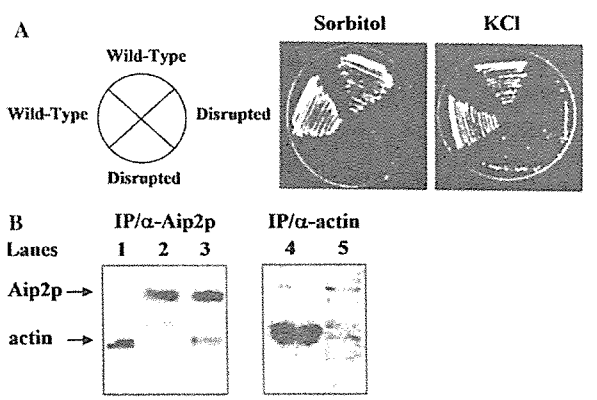

Fig. 3. (A) AIP2-deleted cells are osmotic sensitive. Wild-type (Wild-Type) and AIP2-deleted cells (Disrupted) were grown on rich media containing 1.8 M sorbitol or 1.2 M KCl at 30 °C. (B) Actin and Aip2p were detected by anti-actin antibody (α-actin, lanes 1, 3, and 4) and anti-Aip2p antibody (α-Aip2p, lanes 2, 3, and 5), respectively, in the complex immunoprecipitated with anti-Aip2p antibody (IP/α-Aip2p, lane 3), and in the complex immunoprecipitated with anti-actin antibody (IP/α-actin, lanes 4 and 5). Lanes 1 (actin) and 2 (Aip2p) are marker lanes.

Discussion

A two-hybrid screen originally identified the AIP2 that interacts with actin in *S. cerevisiae* proteins, and therefore it was classified as a member of actin interacting proteins [3]. Chelstowska et al. [1] reported that cell extracts expressing Aip2p exhibited DLD activity in vitro and renamed as D-lactate dehydrogenase protein 2 (Dld2p), even though its expression was not dependent on the Rtg proteins, which are known to be required for the expression of the CIT2 gene that encodes the peroxysomal isoform of citrate synthase. Flick and Konieczny [2] also found Aip2p, implicated with potential MLP/CRP3 interacting proteins, from a mouse cDNA library and exhibited DLD activity in vitro. It is well known that DLD activity is found in mitochondrial fractions. Nevertheless, the interaction between actin cytoskeleton and Aip2p has not been characterized by these efforts.

Given that Aip2p was initially identified as a member of actin interacting protein, several lines of evidence detailing the interaction between Aip2p and actin cytoskeleton were obtained and consisted of: (1) Aip2p-bound F-actin adopted a circular form with a resultant increase in trypsin susceptibility in vitro; (2) rhodamine–phalloidin-stained F-actin congregated in AIP2-deleted cells, however, when Aip2p was overexpressed using a multicopy expression vector, rhodamine–phalloidin-stained F-actin was only sparsely distributed; and (3) AIP2-deleted cells became osmotically sensitive. Schwikowski et al. [16] suggested that the function of Aip2p may be associated with cell polarity by a computational analysis of protein–protein interactions in yeast, which seems to be consistent with our results. It is possible that Dld2p/Aip2p may be multifunctional.

The actin cytoskeleton is relatively flexible compared to microtubules. With regard to in vitro actin manipulation, Ishiwata and colleagues [17] reported a laborious approach that established the formation of a super helix/circular form of F-actin in their motility assay system in which polymerized F-actin was bound to a silicone- or nitrocellulose-coated surface on which a torque component using heavy meromyosin and ATP was assembled to slide F-actin. Even in their well-defined system, formation of the super helix/circular form was determined by chance based on the balance between the magnitude of net torque and the rigidity of the actin filament. Consequently, circular F-actin is not easily produced. In contrast, we achieved the formation of circular F-actin simply by incubating the linear

conformer with Aip2p in the presence of ATP in vitro, a process that was 60–70% efficient over 30 min.

In this study, we have demonstrated that the Aip2p interacts with actin cytoskeleton. Moreover, our results provide the first evidence that Aip2p activity is involved in yeast cell morphology. Disruption or overexpression of the AIP2 significantly affected bud formation in yeast cells, which indicates that Aip2p is required for proper yeast cell morphology. The properties we have identified suggest that a more complete understanding of the activities of Aip2p may facilitate the analysis of the mechanisms that regulate F-actin dynamics in vivo.

Acknowledgments

We greatly thank Y. Kozuka for the technical tutorial and T. Hirai for his assistance. This work was supported by grants from the Core Research for Evolutional Science and Technology (CREST) of Japan Science and Technology Corporation, Health and Labour Sciences Research Grants, Research on Advanced Medical Technology, nano-001, The Naito Foundation, and the Ministry of Health, Labor and Welfare of Japan.

References

[1] A. Chelstowska, Z. Liu, Y. Jia, D. Amberg, R.A. Butow, Signalling between mitochondria and the nucleus regulates the expression of a new D-lactate dehydrogenase activity in yeast, Yeast 15 (1999) 1377–1391.
[2] M.J. Flick, S.F. Konieczny, Identification of putative mammalian D-lactate dehydrogenase enzymes, Biochem. Biophys. Res. Commun. 295 (2002) 910–916.
[3] D.C. Amberg, E. Basart, D. Botstein, Defining protein interactions with yeast actin in vivo, Nat. Struct. Biol. 2 (1995) 28–35.
[4] T.D. Pollard, The cytoskeleton, cellular motility and the reductionist agenda, Nature 422 (2003) 741–745.
[5] A.A. Rodal, J.W. Tetreault, P. Lappalainen, D.G. Drubin, D.C. Amberg, Aip1p interacts with cofilin to disassemble actin filaments, J. Cell Biol. 145 (1999) 1251–1264.
[6] A. Konzok, I. Weber, E. Simmeth, U. Hacker, M. Maniak, A. Muller-Taubenberger, DAip1, a *Dictyostelium* homologue of the yeast actin-interacting protein 1, is involved in endocytosis, cytokinesis, and motility, J. Cell Biol. 146 (1999) 453–464.
[7] W.C. Voegtli, A.Y. Madrona, D.K. Wilson, The structure of Aip1p, A WD repeat protein that regulates cofilin-mediated actin depolymerization, J. Biol. Chem. (2003).
[8] D.C. Amberg, J.E. Zahner, J.W. Mulholland, J.R. Pringle, D. Botstein, Aip3p/Bud6p, a yeast actin-interacting protein that is involved in morphogenesis and the selection of bipolar budding sites, Mol. Biol. Cell 8 (1997) 729–753.
[9] K.R. Ayscough, J. Stryker, N. Pokala, M. Sanders, P. Crews, D.G. Drubin, High rates of actin filament turnover in budding yeast and roles for actin in establishment and maintenance of cell polarity revealed using the actin inhibitor latrunculin-A, J. Cell Biol. 137 (1997) 399–416.
[10] H. Jin, D.C. Amberg, Fission yeast Aip3p (spAip3p) is required for an alternative actin-directed polarity program, Mol. Biol. Cell 12 (2001) 1275–1291.
[11] N. Hachiya, R. Alam, Y. Sakasegawa, M. Sakaguchi, K. Mihara, T. Omura, A mitochondrial import factor purified from rat liver cytosol is an ATP- dependent conformational modulator for precursor proteins, EMBO J. 12 (1993) 1579–1586.
[12] N. Hachiya, T. Komiya, R. Alam, J. Iwahashi, M. Sakaguchi, T. Omura, K. Mihara, MSF, a novel cytoplasmic chaperone which functions in precursor targeting to mitochondria, EMBO J. 13 (1994) 5146–5154.
[13] N. Hachiya, K. Mihara, K. Suda, M. Horst, G. Schatz, T. Lithgow, Reconstitution of the initial steps of mitochondrial protein import, Nature 376 (1995) 705–709.
[14] A.E. Adams, J.R. Pringle, Relationship of actin and tubulin distribution to bud growth in wild-type and morphogenetic-mutant *Saccharomyces cerevisiae*, J. Cell Biol. 98 (1984) 934–945.
[15] P. Novick, D. Botstein, Phenotypic analysis of temperature-sensitive yeast actin mutants, Cell 40 (1985) 405–416.
[16] B. Schwikowski, P. Uetz, S. Fields, A network of protein–protein interactions in yeast, Nat. Biotechnol. 18 (2000) 1257–1261.
[17] T. Nishizaka, T. Yagi, Y. Tanaka, S. Ishiwata, Right-handed rotation of an actin filament in an in vitro motile system, Nature 361 (1993) 269–271.

Available online at www.sciencedirect.com
SCIENCE DIRECT®
Biochemical and Biophysical Research Communications 320 (2004) 1271–1276
BBRC
www.elsevier.com/locate/ybbrc

Oligomeric Aip2p/Dld2p forms a novel grapple-like structure and has an ATP-dependent F-actin conformation modifying activity in vitro

Naomi S. Hachiya,[a,b,c] Yuji Sakasegawa,[a,b] Hiroyuki Sasaki,[d] Akiko Jozuka,[a,b] Shoichiro Tsukita,[b,e] and Kiyotoshi Kaneko[a,c,*]

[a] *Department of Cortical Function Disorders, National Institute of Neuroscience, National Center of Neurology and Psychiatry, Tokyo 187-8502, Japan*
[b] *Tsukita Cell Axis Project, Exploratory Research for Advanced Technology (ERATO) and Solution Oriented Research for Science and Technology (SORST), Japan Science and Technology Corporation, Saitama 332-0012, Japan*
[c] *Core Research for Evolutional Science and Technology (CREST), Japan Science and Technology Agency, Saitama 332-0012, Japan*
[d] *Institute of DNA Medicine, The Jikei University School of Medicine, Tokyo 105-8461, Japan*
[e] *Department of Cell Biology, Faculty of Medicine, Kyoto University, Kyoto 606-8501, Japan*

Received 1 June 2004
Available online 26 June 2004

Abstract

In order to investigate the molecular mechanism of the F-actin conformation modifying activity [Biochem. Biophys. Res. Commun. 319 (2004) 78] of actin-interacting protein 2 (Aip2p) [Nat. Struct. Biol. 2 (1995) 28]/D-lactate dehydrogenase protein 2 (Dld2p) [Yeast 15 (1999) 1377; Biochem. Biophys. Res. Commun. 295 (2002) 910], the ultrastructure and the regulatory mechanism of the activity were further examined. Interestingly, a novel oligomeric grapple-like structure of 10–12 subunits with an ATP-dependent opening was observed. ATP regulates the opening and closing of the "gate" that forms the opening within oligomeric Aip2p/Dld2p, where binding to the substrate occurs while in the open form. In the presence of ATP (open state of oligomeric Aip2p/Dld2p), oligomeric Aip2p/Dld2p bound the F-actin fiber within the opening, whereas in the absence of ATP (closed state of oligomeric Aip2p/Dld2p), no binding was observed. Simultaneously, the oligomeric Aip2p/Dld2p increased the trypsin susceptibility of F-actin in an ATP-dependent manner. Use of the non-hydrolyzable ATP analogue AMP–PNP yielded similar results to those observed with ATP, suggesting that ATP binding rather than ATP hydrolysis is required for the protein conformation modifying reaction of oligomeric Aip2p/Dld2p. Endogenous Aip2p/Dld2p purified from *Saccharomyces cerevisiae* also exhibited such protein conformation modifying activity, but monomeric Aip2p/Dld2p with a C-terminal coiled-coil region-truncation failed to exhibit the activity. These data suggest that the oligomerization of Aip2p/Dld2p, which exhibits the unique grapple-like structure with an ATP-dependent opening, is required for the F-actin conformation modifying activity.

Keywords: Actin interacting protein 2; D-Lactate dehydrogenase protein 2; Oligomeric form; Grapple-like structure; F-actin; Trypsin susceptibility assay; ATP-dependent conformation modifying activity

Actin and its interacting proteins form an indispensable network in cells; a dynamic filament system that is crucial for endocytosis, exocytosis, locomotion, cell division, cytokinesis, shape, and various forms of intracellular motility. Among the actin-interacting proteins, the gene (YDL178w) encoding actin interacting protein 2 (Aip2p) was initially identified using a two-hybrid screen to search for *Saccharomyces cerevisiae* proteins that interact with actin [2]. Subsequently, the YDL178w gene product has been reported to localize on mitochondria and exhibit D-lactate dehydrogenase (DLD) activity in vitro, and therefore renamed as D-lactate dehydrogenase protein 2 (Dld2p) [3]. Besides, Schikowski et al. [5] suggested that the function of Aip2p may be associated with cell polarity by a computational analysis of protein–protein interactions in yeast. Thus, it was possible that Aip2p/Dld2p is multifunctional.

We previously reported that the Aip2p [2]/Dld2p [3,4] exhibits an interaction with F-actin both in vitro and in

* Corresponding author. Fax: +81-42-346-1748.
E-mail address: kaneko@ncnp.go.jp (K. Kaneko).

0006-291X/$ - see front matter © 2004 Elsevier Inc. All rights reserved.
doi:10.1016/j.bbrc.2004.06.082

vivo [1]. Incubation with Aip2p/Dld2p facilitated the formation of the circular form of F-actin in vitro, and the protease susceptibility of the Aip2p/Dld2p-bound "circular form" of F-actin increased, indicating that the Aip2p/Dld2p-bound "circular form" of F-actin possesses an aberrant conformation compared to the linear form of F-actin. When Aip2p/Dld2p was overexpressed in yeast cells, cells produced multibuds from the same mother neck or exhibited elongated bud necks, whereas AIP2-deleted cells displayed deformed morphology reflecting an inability to properly form the cleavage furrow during cell division, which was rescued by the introduction of wild-type Aip2p/Dld2p. While Aip2p/Dld2p-treated F-actin in the circular form was negligibly stained by rhodamine-labeled phalloidin (rhodamine–phalloidin) in vitro, rhodamine–phalloidin staining profiles in actin interacting protein 2 gene (AIP2)-modified cells suggested a correlation between the conformation of F-actin and the expression of Aip2p/Dld2p in vivo. Furthermore, the AIP2-deleted cells became sensitive to an osmotic condition, which is a hallmark of actin dysfunction, and Aip2p/Dld2p co-immunoprecipitated with actin in yeast cells. These properties suggest that Aip2p/Dld2p interacts with F-actin both in vitro and in vivo and plays an important role in the yeast cell morphology.

Under the background, here we further characterized the F-actin conformation modifying activity of Aip2p/Dld2p in terms of the ultrastructure and the regulatory mechanism of such activity. As results, we revealed that the activity requires a unique oligomeric grapple-like structure of 10–12 subunits with an ATP-dependent opening.

Materials and methods

Yeast strain and antibody. Wild-type yeast strains (ATCC24657) used in this study were purchased from American Type Culture Collection. Protease deficient strain SH2777 was a gift from Dr. Harashima, Osaka University. A synthetic peptide corresponding to the C-terminal 15 amino-acid residues of Aip2p/Dld2p (VHYDPNGILNPYKYI) was coupled through a COOH-terminal cysteine residue to BSA, and antibody was affinity purified using the antigen.

Trypsin susceptibility assay. The trypsin susceptibility assay was performed as previously described [1,6–8]. Briefly, assays (200 μl) were initiated by adding 200 ng of polymerized rabbit muscle actin to buffer A (10 mM Tris–Cl, pH 8.0, 0.1 M KCl, and 10 mM $MgCl_2$) containing 1 mM ATP and 500 ng of hexahistidine-tagged Aip2p/Dld2p, and incubated at 30 °C for 15 min. After incubation, samples were treated with trypsin (0.2 μg ml^{-1}) at 16 °C for 15 min. The reaction was terminated by incubation with soybean trypsin inhibitor (0.4 μg ml^{-1}) on ice for 5 min, TCA-precipitated with tRNA carrier, and then subjected to SDS–PAGE and Western blotting. To detect actin, affinity-purified polyclonal rabbit anti-actin antibody served as the primary antibody and horseradish peroxidase-linked IgG (ICN Pharmaceuticals) was the secondary antibody. Immunoreactive bands were visualized by ECL-plus (Amersham Biosciences) and analyzed using a Fluoro Smax (Bio-Rad).

Purification of hexahistidine-tagged Aip2p/Dld2p. In an effort to obtain sufficient quantities of Aip2p/Dld2p, the protein was prepared from the expression strain in yeast under control of the ADH promoter as previously described [1]. Briefly, the C-terminally hexahistidine-tagged YDL178w gene was amplified by PCR and inserted into the aureobasidin A (Ab A) selective expression vector pAUR123 (TaKaRa Biomedicals). The protease deficient strain SH2777 was transformed by this plasmid and transformants were grown on YPD plates containing 0.5 μg ml^{-1} Ab A. Inoculated medium (8 L) was incubated overnight at 30 °C to an OD at 600 nm of 1–2. Cells were collected, resuspended in four volumes of buffer B (50 mM NaPi, pH 8.0, 150 mM NaCl, and 10 mM imidazole), crushed using glass beads, and centrifuged at 10,000 rpm for 10 min at 4 °C. Supernatants were collected and ultracentrifuged at 100,000*g* at 4 °C for 1 h. The precipitate was resuspended, passed through a Ni–NTA agarose column (Qiagen, K.K.) equilibrated in buffer B, and subsequently eluted with buffer B containing 0.5 M imidazole. Eluted fractions were dialyzed against buffer C (10 mM Hepes–KOH, pH 7.4, 50 mM NaCl, and 1 mM DTT), applied to an ion exchange Mono Q column (Amersham–Pharmacia Biotech, AKTA System) equilibrated with buffer C, and eluted with a linear NaCl gradient (100–500 mM). Immunoreactive fractions were dialyzed against buffer D (50 mM NaPi, pH 7.5, 10 mM NaCl, and 1 mM Mg $(OAc)_2$), and finally passed through a Superdex 200 gel filtration column equilibrated with buffer D.

C-terminal coiled-coil domain-truncated Aip2p/Dld2p. To generate C-terminal coiled-coil domain-truncated Aip2p/Dld2p, the gene for the C-terminal 100 amino acid residue-truncated form of C-terminally hexahistidine-tagged Aip2p/Dld2p was amplified by PCR and inserted into the yeast expression vector pAUR123 (TaKaRa Biomedicals). The Aip2p/Dld2p-deleted strain was transformed by this plasmid, and transformants were checked by colony PCR, selected on YPD plates containing 500 ng ml^{-1} Ab A, inoculated, and the protein was finally purified.

Purification of endogenous Aip2p/Dld2p. Yeast microsome fraction from the yeast strain ATCC 24657 [MATα mal [rho+]CAN^S] (25 L) was incubated with buffer E (10 mM Hepes–KOH, pH 7.4, 1 mM DTT, and 1 mM $Mg(OAc)_2$) containing 500 mM NaCl on ice for 20 min and then centrifuged at 100,000*g* for 60 min at 4 °C. Following centrifugation, the salt-extracted fraction was dialyzed against buffer E overnight at 4 °C, passed through DEAE–Sepharose Fast Flow (Amersham Biosciences) equilibrated with buffer E, washed with 50 mM NaCl, and then eluted with 300 mM NaCl. The eluate was dialyzed against buffer E, passed through Resource Q (Amersham Biosciences), and eluted with a linear NaCl gradient (100–500 mM). Active fractions were further purified using hydroxyapatite (Seikagaku Kogyo) and ATP agarose (Sigma).

Results

In an effort to examine the structure of Aip2p/Dld2p by electron microscopy, we cloned the YDL178W gene and expressed it in yeast cells under control of the ADH promoter using an Ab A expression system (TAKARA, BIO) to yield highly purified protein [1]. Electron microscopic observation of purified Aip2p/Dld2p using rotary shadowing method [9] revealed that it possesses an unusual "grapple-like" oligomeric structure of ~10 nm in diameter within the opening (Fig. 1A, left panels). Furthermore, negative staining observation [10] revealed that oligomeric Aip2p/Dld2p adopted at least two different states that corresponded to an "open state" in the presence of ATP, or a "closed state" in the absence of ATP (Fig. 1A, right panels). Aip2p/Dld2p contains two ATP-binding Walker type B motifs

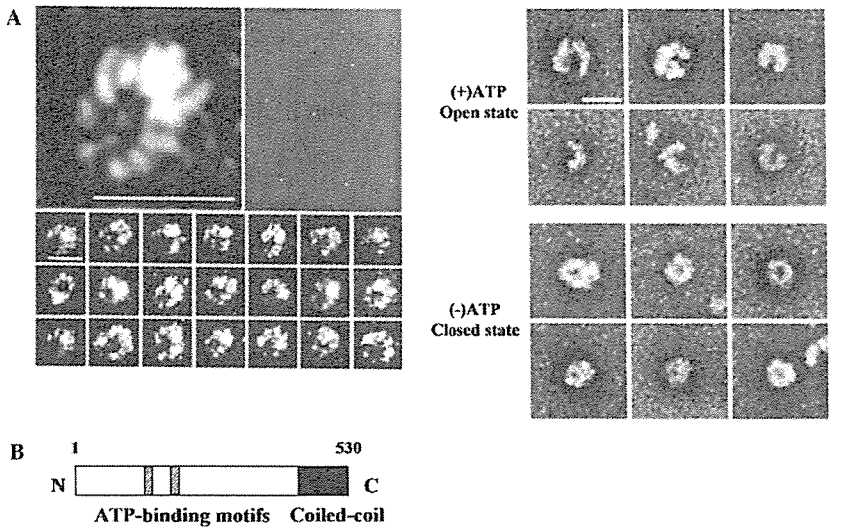

Fig. 1. A grapple-like oligomeric structure of Aip2p/Dld2p. (A) Left panels: purified hexahistidine-tagged oligomeric Aip2p/Dld2p (100 μg ml^{-1}) was used as a specimen for low angle shadowing electron microscopy. Scale bars are 10 nm. Right panels: negative staining of oligomeric Aip2p/Dld2p in the "open state" and "closed state." In the presence of ATP, oligomeric Aip2p/Dld2p opens its opening ((+)ATP) and without ATP the opening is closed ((−)ATP). Scale bar is 10 nm. (B) Schematic representation of the structure of YDL178W [2] encoding Aip2p/Dld2p. Two ATP-binding Walker type B motifs (ZZZZD, where Z is a hydrophobic residue) [11] locate at amino acid residues from 142 to 146 and 189 to 193 (hatched), and a coiled-coil domain locates in its C-terminal 100 amino acid residues (filled) [12].

(ZZZZD, where Z is a hydrophobic residue) [11] located at amino acid residues from 142 to 146 and 189 to 193, which are conserved among several Mg^{2+}-nucleotide binding proteins (Fig. 1B).

Gel filtration chromatography was then performed in order to determine the number of Aip2p/Dld2p monomers present in the oligomeric complex. Oligomeric Aip2p/Dld2p eluted as a single peak with an apparent molecular weight of ~700 kDa (Fig. 2A). Given that the molecular weight of Aip2p/Dld2p in the monomeric form was about ~60 kDa [1], it is apparent that Aip2p/Dld2p forms an oligomeric structure consisting of 10–12 subunits. Secondary structure prediction [12] indicated that Aip2p/Dld2p contains a coiled-coil domain in its C-terminal region (Fig. 1B). To determine the functional significance of this region in relation to oligomerization, coiled-coil region-deleted recombinant Aip2p/Dld2p was expressed and purified from yeast cells. As shown in Fig. 2B, C-terminal-truncated Aip2p/Dld2p eluted at an apparent molecular weight of ~60 kDa, indicating that Aip2p/Dld2p oligomerization occurs via the C-terminal coiled-coil region. Next, the protease susceptibility assay was employed to examine the conformation modifying activity of the coiled-coil domain-deleted monomeric form of Aip2p/Dld2p. This truncated monomeric form of Aip2p/Dld2p did not possess F-actin conformation modifying activity, as suggested by the result that its trypsin susceptibility was not affected even in the presence of ATP (Fig. 2C).

In addition to the aforementioned indirect biochemical analyses suggesting that oligomeric Aip2p/Dld2p possesses F-actin conformation modifying activity, more direct evidence of this activity was sought through the use of low angle rotary shadowing [9]. Following incubation of rabbit muscle F-actin with oligomeric Aip2p/Dld2p in the presence of ATP (open state of Aip2p/Dld2p), oligomeric Aip2p/Dld2p bound the F-actin fiber within the opening (Fig. 3A, (+)ATP), whereas in the absence of ATP (closed state of Aip2p/Dld2p), given that the opening was closed, no binding was observed (Fig. 3A, (−)ATP). Previously, we reported that incubation with Aip2p/Dld2p facilitated the formation of the circular form of F-actin in vitro, which exhibited an aberrant trypsin susceptibility [1]. However, the radius of this circular F-actin was 2–4 μm on average and was not detectable under the electron microscope at higher magnification (100,000×) used in this study. Consistent with these results, oligomeric Aip2p/Dld2p increased the trypsin susceptibility of F-actin in the presence of ATP (Fig. 3B, (+)ATP). Use of the non-hydrolyzable ATP analogue AMP–PNP yielded similar results to those observed with ATP (Fig. 3B, (+)AMP–PNP), whereas the use of ADP failed to alter the trypsin susceptibility of F-actin (Fig. 3B, (+)ADP). These data suggested that ATP binding rather than ATP hydrolysis is required for the protein conformation modifying reaction of oligomeric Aip2p/Dld2p.

The trypsin susceptibility assay was further applied to isolate the F-actin conformation modifying activity in yeast cells in vivo. Several steps consisting of ion exchange chromatography followed by affinity chromatography with ATP–agarose facilitated the purification to homogeneity of endogenous Aip2p/Dld2p, of which the identity was confirmed by amino acid sequence

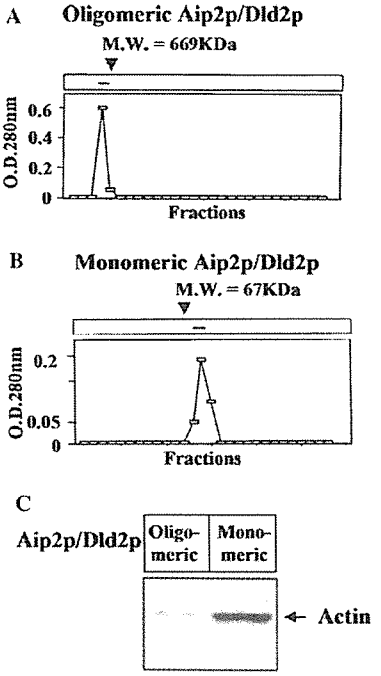

Fig. 2. Oligomeric Aip2p/Dld2p exhibits F-actin conformation modifying activity. (A) Gel filtration chromatography (Superdex 200 column, Amersham BioSciences, Smart system) was performed with purified hexahistidine-tagged full-length Aip2p/Dld2p in oligomeric form. Thyroglobulin (molecular weight (MW) = 669 kDa) was used as a marker protein. (B) The C-terminal coiled-coil region-truncated Aip2p/Dld2p eluted as a monomeric protein. Bovine serum albumin (MW = 67 kDa) was used as a marker protein. (C) The coiled-coil region-truncated monomeric Aip2p/Dld2p possesses no protein conformation modifying activity. Two micromolar of rabbit muscle actin (Molecular Probes) was polymerized in the high salt buffer (10 mM Tris–Cl, pH 8.0, 100 mM KCl, and 2 mM $MgCl_2$) at 37 °C for 2 h. Oligomeric and monomeric forms of Aip2p/Dld2p were purified and incubated with the polymerized rabbit muscle actin in the presence of 1 mM ATP and the trypsin susceptibility assay was performed.

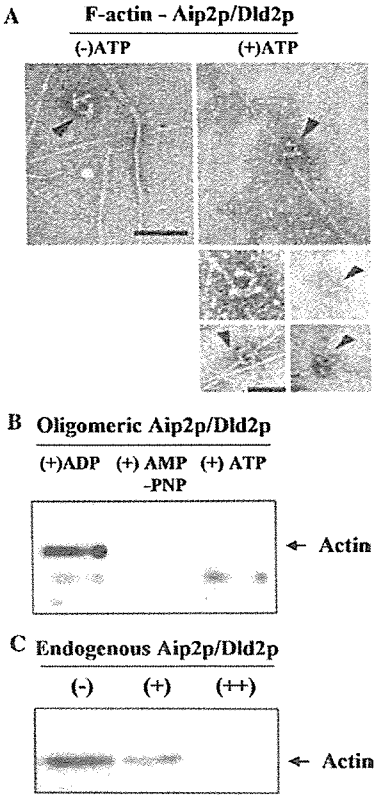

Fig. 3. F-actin binding and conformation modifying activity of oligomeric Aip2p/Dld2p are ATP-dependent. (A) Two hundred micrograms of polymerized rabbit muscle actin (see legend to Fig. 2C) was incubated with or without 500 μg of oligomeric Aip2p/Dld2p in the presence or absence of 1 mM ATP and then examined by negative staining (100,000×). Scale bars are 20 nm. In the presence of ATP, oligomeric Aip2p/Dld2p (arrowheads) binds to F-actin in the opening. (B) The same reaction mixture was subjected to the trypsin susceptibility assay. F-actin (200 ng) and oligomeric Aip2p/Dld2p (500 ng) were incubated in buffer E with 1 mM ATP ((+)ATP), 1 mM AMP–PNP ((+)AMP–PNP) or 1 mM ADP ((+)ADP). In the presence of ATP ((+)ATP) or AMP–PNP ((+)AMP–PNP), oligomeric Aip2p/Dld2p modifies the trypsin susceptibility of F-actin. Endogenous Aip2p/Dld2p purified from *S. cerevisiae* exhibits actin conformation modifying activity. (C) Endogenous Aip2p/Dld2p (–) represents the trypsin-protected control band. (+)/(++) refers to 300/500 ng of endogenous Aip2p/Dld2p. Protected bands were detected by Western blotting using polyclonal antibodies against actin and visualized with ECL-plus. Endogenous Aip2p/Dld2p alters the trypsin susceptibility of actin in a dose-dependent manner.

analysis (see Materials and methods). Low concentrations of trypsin did not digest actin (Fig. 3C, (–)). However, when endogenous Aip2p/Dld2p purified from *S. cerevisiae* was added and incubated for 15 min at 30 °C, the previously protected band decreased in intensity depending on the amount of extract added (Fig. 3C, (+) and (++)). Given the fact that truncated monomeric form of Aip2p/Dld2p does not possess F-actin conformation modifying activity, the purified Aip2p/Dld2p is likely to be an oligomeric form.

Discussion

Oligomeric Aip2p/Dld2p forms an unusual "grapple-like" structure

Given that structural analysis can provide details concerning the molecular profiles of targets, the ultrastructure of oligomeric Aip2p/Dld2p was visualized directly using low angle rotary shadowing electron microscopy. This revealed a grapple-like oligomeric structure of ~10 nm in diameter within the opening. In the presence of ATP, oligomeric Aip2p/Dld2p bound F-actin in the opening through its unique "grapple-like" structure, which is quite unprecedented. F-actin entered and was caught in the grapple-shaped opening, where its conformation was modified in the presence of ATP. On the other hand, in the absence of ATP or in the presence

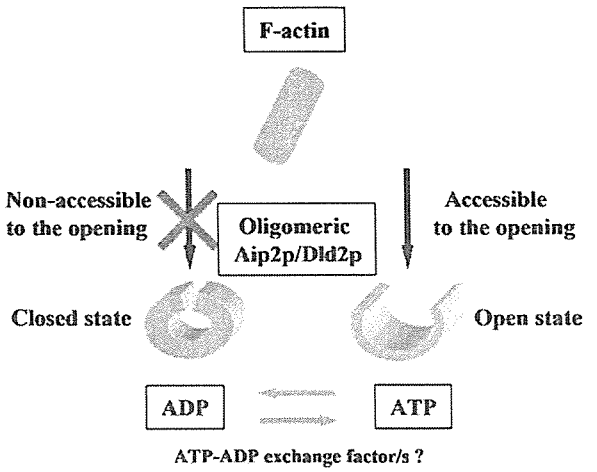

Fig. 4. The ATP-dependent open and closed state model of oligomeric Aip2p/Dld2p. ATP-bound oligomeric Aip2p/Dld2p exhibits a protein conformation modifying activity (open state), whereas F-actin is unable to penetrate ATP-unbound oligomeric Aip2p/Dld2p (closed state).

of ADP, the opening was closed, and thus F-actin could not enter the opening (Fig. 4). Consistent with this observation, monomeric Aip2p/Dld2p with a C-terminal coiled-coil region-truncation failed to exhibit the protein conformation modifying activity.

The structures and functions of Hsp70 family proteins and chaperonins have been extensively investigated [13,14]. DnaK binds short peptides bearing a core of hydrophobic residues to its cleft with a lid, the opening and closing of which is mediated via the ATPase domain [15]. Group I chaperonins generally form homoheptameric rings stacked back-to-back to yield a cylinder possessing two central cavities. GroEL, with conserved hydrophobic residues that are aligned along the cylinder opening on the apical domains, recognizes and binds hydrophobic surfaces of nonnative proteins [16]. ATP-binding and the dome-shaped cofactor, GroES, displace the bound substrate from within the GroEL cavity, where folding is facilitated by preventing aggregation [17]. Group II chaperonins, GimC/prefoldin, TRiC/CCT, and thermosome are not homologous to Group I chaperonins but share a similar overall architecture. They form homo-oligomeric rings of 8–9 subunits and function without a GroES-like capping cofactor [15,18]. They apparently rely on α-helical extensions of their apical domains that are thought to mediate opening and closing of their folding chamber and have a "built-in" lid.

While these chaperonins are composed of similar oligomeric structures within the central cavity, oligomeric Aip2p/Dld2p is clearly distinct with a grapple-like structure of 10–12 subunits that can modify the conformation of substrate. When interactions between the conventional chaperonins and long fibrous substrates such as F-actin are considered, oligomeric Aip2p/Dld2p may outperform the ring- or cylinder-shaped conventional chaperonins, since with the latter, either end has to be dragged in and then passed through the central cavity all the way. In contrast, a grapple-like structure in the "open state" is able to bind targets, such long fibers, directly at any point, even in the middle.

Oligomeric Aip2p/Dld2p exhibits an ATP-dependent F-actin conformation modifying activity

It was found that oligomeric Aip2p/Dld2p exhibited an F-actin conformation modifying activity, which is regulated by the binding of ATP to oligomeric Aip2p/Dld2p. It has been well documented that the activity of hsp70 proteins is regulated by two co-chaperones, DnaJ homologues that stimulate ATP hydrolysis [19,20], and GrpE that mediates the ATP–ADP exchange reaction [21,22]. Although the reaction mechanism associated with oligomeric Aip2p/Dld2p is clearly distinct from hsp70, we are tempted to speculate that a similar factor/s may function as co-chaperone/s to regulate ATP-hydrolysis or ATP–ADP exchange in the protein conformation modification cycle. Actually, the protein conformation modifying activity is regulated by the binding of ATP to oligomeric Aip2p/Dld2p, but not by ATP hydrolysis according to the current experimental result with non-hydrolyzable ATP analogue, AMP–PNP. Consistent with this notion, partially purified Aip2p/Dld2p at the log phase possessed higher protein conformation modifying activity and ATP-binding capacity than those of Aip2p/Dld2p purified at the stationary phase, suggesting the presence of a cofactor/s that may provide ATP to Aip2p/Dld2p (Hachiya et al., unpublished data).

Finally, it is important to clarify if the oligomeric Aip2p/Dld2p exclusively binds and modifies F-action conformation. Although it is very preliminary, our data suggested that the oligomeric Aip2p/Dld2p also bound and modified the conformation of DNase I, the mature form of invertase, mitochondrial SOD, and heavy meromyosin, as determined by the trypsin susceptibility assay (data not shown). Clearly, more detailed examination especially on its substrate specificity in vivo has yet to be done.

These data may support the notion that the oligomeric Aip2p/Dld2p may belong to an unusual class of molecular chaperones, which exhibits the unique grapple-like structure with an ATP-dependent opening. Whether such activity is exceptional or forms a novel class of molecular chaperones remains to be determined.

Acknowledgments

We are indebted to G. Schatz, S.B. Prusiner, K. Mihara, and R. Scheckman for critical discussions and to I. Wada, N. Hoogenraad, M. Ryan, and A. Asano for helpful comments. We are also grateful to Y.

Kozuka, K. Ihara, S. Yoshioka, M. Yamada, K. Watanabe, E.A. Nannri, and K. Ishibashi for technical assistance. This work was supported in part by grants from the Ministry of Health, Labor and Welfare of Japan, Exploratory Research for Advanced Technology (ERATO) and Core Research for Evolutional Science and Technology (CREST) of the Japan Science Technology Corporation (JST), Health and Labour Sciences Research Grants, Research on Advanced Medical Technology, nano-001, the Ministry of Health, Labour and Welfare of Japan, and the Naito Foundation.

References

[1] N.S. Hachiya, Y. Sakasegawa, A. Jozuka, S. Tsukita, K. Kaneko, Interaction of D-lactate dehydrogenase protein 2 (Dld2p) with F-actin: implication for an alternative function of Dld2p, Biochem. Biophys. Res. Commun. 319 (2004) 78–82.

[2] D.C. Amberg, E. Basart, D. Botstein, Defining protein interactions with yeast actin in vivo, Nat. Struct. Biol. 2 (1995) 28–35.

[3] A. Chelstowska, Z. Liu, Y. Jia, D. Amberg, R.A. Butow, Signalling between mitochondria and the nucleus regulates the expression of a new D-lactate dehydrogenase activity in yeast, Yeast 15 (1999) 1377–1391.

[4] M.J. Flick, S.F. Konieczny, Identification of putative mammalian D-lactate dehydrogenase enzymes, Biochem. Biophys. Res. Commun. 295 (2002) 910–916.

[5] B. Schwikowski, P. Uetz, S. Fields, A network of protein–protein interactions in yeast, Nat. Biotechnol. 18 (2000) 1257–1261.

[6] N. Hachiya, R. Alam, Y. Sakasegawa, M. Sakaguchi, K. Mihara, T. Omura, A mitochondrial import factor purified from rat liver cytosol is an ATP-dependent conformational modulator for precursor proteins, EMBO J. 12 (1993) 1579–1586.

[7] N. Hachiya, T. Komiya, R. Alam, J. Iwahashi, M. Sakaguchi, T. Omura, K. Mihara, MSF, a novel cytoplasmic chaperone which functions in precursor targeting to mitochondria, EMBO J. 13 (1994) 5146–5154.

[8] N. Hachiya, K. Mihara, K. Suda, M. Horst, G. Schatz, T. Lithgow, Reconstitution of the initial steps of mitochondrial protein import, Nature 376 (1995) 705–709.

[9] S. Tsukita, Desmocalmin: a calmodulin-binding high molecular weight protein isolated from desmosomes, J. Cell Biol. 101 (1985) 2070–2080.

[10] Y. Nonomura, E. Katayama, S. Ebashi, Effect of phosphates on the structure of the actin filament, J. Biochem. (Tokyo) 78 (1975) 1101–1104.

[11] J.E. Walker, M. Saraste, M.J. Runswick, N.J. Gay, Distantly related sequences in the alpha- and beta-subunits of ATP synthase, myosin, kinases and other ATP-requiring enzymes and a common nucleotide binding fold, EMBO J. 1 (1982) 945–951.

[12] A. Lupas, M. Van Dyke, J. Stock, Predicting coiled coils from protein sequences, Science 252 (1991) 1162–1164.

[13] F.U. Hartl, Molecular chaperones in cellular protein folding, Nature 381 (1996) 571–580.

[14] S. Walter, J. Buchner, Molecular chaperones—cellular machines for protein folding, Angew. Chem. Int. Ed. Engl. 41 (2002) 1098–1113.

[15] M.P. Mayer, H. Schroder, S. Rudiger, K. Paal, T. Laufen, B. Bukau, Multistep mechanism of substrate binding determines chaperone activity of Hsp70, Nat. Struct. Biol. 7 (2000) 586–593.

[16] W.A. Houry, Mechanism of substrate recognition by the chaperonin GroEL, Biochem. Cell. Biol. 79 (2001) 569–577.

[17] J.S. Weissman, C.M. Hohl, O. Kovalenko, Y. Kashi, S. Chen, K. Braig, H.R. Saibil, W.A. Fenton, A.L. Horwich, Mechanism of GroEL action: productive release of polypeptide from a sequestered position under GroES, Cell 83 (1995) 577–587.

[18] A.S. Meyer, J.R. Gillespie, D. Walther, I.S. Millet, S. Doniach, J. Frydman, Closing the folding chamber of the eukaryotic chaperonin requires the transition state of ATP hydrolysis, Cell 113 (2003) 369–381.

[19] T. Laufen, M.P. Mayer, C. Beisel, D. Klostermeier, A. Mogk, J. Reinstein, B. Bukau, Mechanism of regulation of hsp70 chaperones by DnaJ cochaperones, Proc. Natl. Acad. Sci. USA 96 (1999) 5452–5457.

[20] R. Russell, A. Wali Karzai, A.F. Mehl, R. McMacken, DnaJ dramatically stimulates ATP hydrolysis by DnaK: insight into targeting of Hsp70 proteins to polypeptide substrates, Biochemistry 38 (1999) 4165–4176.

[21] Y. Groemping, D. Klostermeier, C. Herrmann, T. Veit, R. Seidel, J. Reinstein, Regulation of ATPase and chaperone cycle of DnaK from *Thermus thermophilus* by the nucleotide exchange factor GrpE, J. Mol. Biol. 305 (2001) 1173–1183.

[22] J.P. Grimshaw, I. Jelesarov, H.J. Schonfeld, P. Christen, Reversible thermal transition in GrpE, the nucleotide exchange factor of the DnaK heat-shock system, J. Biol. Chem. 276 (2001) 6098–6104.

Available online at www.sciencedirect.com
SCIENCE DIRECT®
Biochemical and Biophysical Research Communications 323 (2004) 339–344
BBRC
www.elsevier.com/locate/ybbrc

Oligomeric Aip2p/Dld2p modifies the protein conformation of both properly folded and misfolded substrates in vitro

Naomi S. Hachiya[a,b,c], Yuji Sakasegawa[a,b], Hiroyuki Sasaki[d], Akiko Jozuka[a,b], Shoichiro Tsukita[b,e], Kiyotoshi Kaneko[a,c,*]

[a] *Department of Cortical Function Disorders, National Institute of Neuroscience, National Center of Neurology and Psychiatry, Tokyo 187-8502, Japan*
[b] *Tsukita Cell Axis Project, Exploratory Research for Advanced Technology (ERATO) and Solution Oriented Research for Science and Technology (SORST), Japan Science and Technology Corporation, Saitama 332-0012, Japan*
[c] *Core Research for Evolutional Science and Technology (CREST), Japan Science and Technology Agency, Saitama 332-0012, Japan*
[d] *Institute of DNA Medicine, The Jikei University School of Medicine, Tokyo 105-8461, Japan*
[e] *Department of Cell Biology, Faculty of Medicine, Kyoto University, Kyoto 606-8501, Japan*

Received 7 August 2004

Abstract

Oligomeric actin-interacting protein 2 (Aip2p) [Nat. Struct. Biol. 2 (1995) 28]/D-lactate dehydrogenase protein 2 (Dld2p) [Yeast 15 (1999) 1377, Biochem. Biophys. Res. Commun. 295 (2002) 910] exhibits the unique grapple-like structure with an ATP-dependent opening [Biochem. Biophys. Res. Commun. 320 (2004) 1271], which is required for the F-actin conformation modifying activity in vitro and in vivo [Biochem. Biophys. Res. Commun. 319 (2004) 78]. To further investigate the molecular nature of oligomeric Aip2p/Dld2p, the substrate specificity of its binding and protein conformation modifying activity was examined. In the presence of 1 mM ATP or AMP-PNP, oligomeric Aip2p/Dld2p bound to all substrates so far examined, and modified the conformation of actin, DNase I, the mature form of invertase, prepro-α-factor, pro-α-factor, and mitochondrial superoxide dismutase, as determined by the trypsin susceptibility assay. Of note, the activity could modify even the conformation of pathogenic highly aggregated polypeptides, such as recombinant prion protein in β-sheet form, α-synuclein, and amyloid β (1–42) in the presence of ATP. The in vivo protein conformation modifying activity, however, depends on the growth stage; the most significant substrate modification activity was observed in yeast cells at the log phase, suggesting the presence of a cofactor/s in yeast cells, where F-actin is supposed to be a major target in vivo. These data further support our previous notion that the oligomeric Aip2p/Dld2p may belong to an unusual class of molecular chaperones [Biochem. Biophys. Res. Commun. 320 (2004) 1271], which can target both properly folded and misfolded proteins in an ATP-dependent manner in vitro.

Keywords: Actin interacting protein 2; D-Lactate dehydrogenase protein 2; Oligomeric form; Trypsin susceptibility assay; ATP-dependent conformation modifying activity; Broad substrate specificity; β-Sheet conformation; Cell-cycle dependent

The actin and its interacting proteins play diverse roles in the cell, mediating endocytosis, exocytosis, cell motility, cell polarity, and cytokinesis [6]. Among them, a search for *Saccharomyces cerevisiae* proteins that interact with actin in the two-hybrid system identified the gene encoding Aip2p (YDL178w) [1], and the same gene product has been reported to exhibit D-lactate dehydrogenase (DLD) activity in vitro in yeast cells [2] as well as in mammalian cells [3].

We previously reported that the Aip2p [1]/Dld2p [2,3] exhibits an interaction with F-actin both in vitro and in vivo with its unique grapple-like structure and an ATP-dependent opening [5]. Incubation with Aip2p/Dld2p

* Corresponding author. Fax: +81 42 346 1748.
E-mail address: kaneko@ncnp.go.jp (K. Kaneko).

0006-291X/$ - see front matter © 2004 Elsevier Inc. All rights reserved.
doi:10.1016/j.bbrc.2004.08.098

facilitated the formation of the circular form of F-actin in vitro, which possessed an aberrant conformation compared to the linear form of F-actin. Overexpression of Aip2p induced multi-buds in yeast cells, whereas reduced expression interfered with the formation of the cleavage furrow for the cell division, which was rescued by the introduction of wild-type Aip2p. While Aip2p-treated F-actin in the circular form was negligibly stained by rhodamine-labeled phalloidin (rhodamine–phalloidin) in vitro, rhodamine–phalloidin staining profiles in actin interacting protein 2 gene (AIP2)-modified cells suggested a correlation between the conformation of F-actin and the expression of Aip2p in vivo. Furthermore, the AIP2-deleted cells became sensitive to an osmotic condition, which is a hallmark of actin dysfunction, and Aip2p/Dld2p co-immunoprecipitated with actin in yeast cells.

Following ultrastructural analysis revealed a novel oligomeric grapple-like structure of 10–12 subunits with an ATP-dependent opening [4]. ATP regulates the opening and closing of the "gate" that forms the opening within oligomeric Aip2p/Dld2p, where binding to the substrate occurs while in the open form. In the presence of ATP (open state), oligomeric Aip2p/Dld2p bound the F-actin fiber within the opening, whereas in the absence of ATP (closed state), no binding was observed. Simultaneously, the oligomeric Aip2p/Dld2p increased the trypsin susceptibility of F-actin in an ATP-dependent manner that ATP-binding rather than ATP hydrolysis is required for the protein conformation modifying reaction.

During our consecutive investigation, it was suggested that the oligomeric Aip2p/Dld2p also bound and modified the conformation of several protein substrates other than F-actin as determined by the trypsin susceptibility assay in vitro. Here, we further examined the substrate specificity of its binding property and protein conformation modifying activity. Of note, the oligomeric Aip2p/Dld2p could target both properly folded and even pathogenic highly aggregated proteins and thus, it exhibited no obvious substrate specificity for its binding and robust protein conformation modifying activity in vitro.

Materials and methods

Yeast strain and antibodies. Protease deficient strain SH2777 was a gift from Dr. Harashima, Osaka University. Affinity-purified polyclonal rabbit anti-actin, anti-α-synuclein, and anti-heavy meromyosin (HMM) antibodies were purchased from Chemicon. Anti-cytochrome *c* antibody was purchased from BD Biosciences. Anti-SOD and anti-DNase I antibodies were purchased from Sigma Chemical. Affinity-purified polyclonal rabbit anti-invertase and anti-α-factor antibodies were raised against polypeptides harbouring 15 amino acid residues at the C-terminus, respectively. Anti-recombinant prion protein (PrP) antibody, K1, was rabbit polyclonal antibody raised against PrP residues 26–40 [7,8].

Preparation of substrate proteins. Amyloid β (1–28), amyloid β (1–42), cytochrome *c*, DNase I, malate dehydrogenase (MDH), and mitochondrial SOD were purchased from Sigma Chemical. α-Synuclein was purchased from Chemicon. HMM, luciferase, and the mature form of invertase were purchased from Wako Chemicals. Rabbit muscle actin was purchased from Molecular Probes. Two micromolar of rabbit muscle G-actin was polymerized in high salt buffer (10 mM Tris–Cl, pH 8.0, 100 mM KCl, and 2 mM $MgCl_2$) at 37 °C for 2 h, and used as F-actin. The gene fragments of hexahistidine-tagged ppαF and proαF were amplified by PCR, respectively, inserted into pET11a plasmid, expressed in *Escherichia coli* BL21(DE3) using the pET system, and purified according to the manufacturer's protocol (Qiagen, K.K.). Purified ppαF was dialyzed against buffer A (10 mM Hepes–KOH, pH 7.4, 1 mM DTT, and 1 mM $Mg(OAc)_2$) and subsequently used in the trypsin susceptibility protein conformation modifying assay. Recombinant PrP (rPrP) was purchased from Prionics, AG. The PrP solubilized in PBS was kept at 4 °C until circular dichroism detected over 50% of β-sheet contents in the rPrP, and then used as "PrP in β-sheet form."

Surface plasmon resonance. BIAcore 3000 system was used to analyze molecular interactions by means of surface plasmon resonance (SPR). Purified oligomeric form of Aip2p/Dld2p was covalently linked to a Sensor Chip CM5 (carboxymethylated dextran surface), with the use of amine coupling chemistry according to manufacturer's instructions. Samples for analyte proteins were diluted (10 μg ml^{-1}) in the running buffer (10 mM Hepes–KOH, pH 7.4, 150 mM NaCl, 1 mM $MgCl_2$, 3 mM EDTA, 0.005% surfactant P20, and 1 mM ATP), and injected over the surface at 4 °C with a flow rate of 5 μl min^{-1}. Each sensorgram was subtracted for the response observed in the control flow cell containing a blank surface and results were analyzed by using BIA evaluation SPR kinetic software (Biacore).

Purification of hexahistidine-tagged Aip2p/Dld2p and trypsin susceptibility assay. In an effort to obtain sufficient quantities of oligomeric Aip2p/Dld2p, the protein was prepared from the expression strain in yeast under control of the ADH promoter as previously described [4,5]. The trypsin susceptibility assay was performed as previously described [4,5,9–11]. Briefly, assays (200 μl) were initiated by adding 200 ng (if not indicated) of protein substrates to buffer B (10 mM Tris–Cl, pH 8.0, 0.1 M KCl, and 10 mM $MgCl_2$) containing 1 mM ATP and 500 ng of hexahistidine-tagged oligomeric Aip2p/Dld2p, and incubated at 30 °C for 15 min. After incubation, samples were treated with trypsin (0.2 μg ml^{-1}) at 16 °C for 15 min. The reaction was terminated by incubation with soybean trypsin inhibitor (0.4 μg ml^{-1}) on ice for 5 min, TCA-precipitated with tRNA carrier, and then subjected to SDS–PAGE and Western blotting with corresponding antibody at 1:1000 (unless otherwise noted). Immunoreactive bands were visualized by ECL-plus (Amersham Biosciences) and analyzed using a Fluoro SMAX (Bio-Rad).

Results

Substrate recognition and binding of oligomeric Aip2p/Dld2p

To examine the in vitro oligomeric Aip2p/Dld2p-substrate-binding specificity in detail, we performed a surface plasmon resonance (SPR) assay with a wide variety of proteins as binding substrates including amyloid β (1–28), amyloid β (1–42), α-synuclein, cytochrome *c*, F-actin, G-actin, HMM, Invertase, MDH, ppαF, proαF, PrP, and SOD. In the presence of 1 mM ATP (see Fig. 1A) or AMP-PNP (data not shown), oligomeric Aip2p/Dld2p bound to all substrates so far exam-

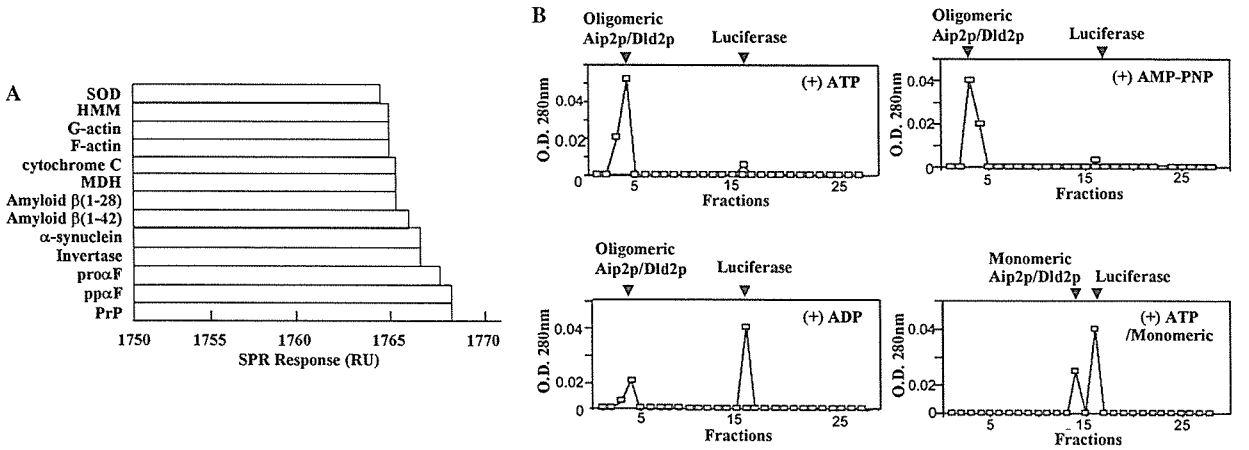

Fig. 1. Oligomeric Aip2p/Dld2p binds to all substrates examined in an ATP-dependent manner. (A) Interactions between oligomeric Aip2p/Dld2p and substrate proteins were measured by surface plasmon resonance (SPR) assay in the presence of ATP (see Materials and methods). SOD, superoxide dismutase; HMM, heavy meromyosin; MDH, malate dehydrogenase; proαF, pro-α-factor; ppαF, prepro-α-factor; and PrP, recombinant prion protein. (B) ATP requirement for its substrate-binding activity. Luciferase (300 ng) and oligomeric Aip2p/Dld2p (100 ng) were incubated in buffer B (see Materials and methods) with 1 mM ATP ((+) ATP), 1 mM AMP-PNP ((+) AMP-PNP), or 1 mM ADP ((+) ADP). Truncated monomeric Aip2p/Dld2p [4] could not bind substrate even in the presence of ATP ((+) ATP/monomeric). Each sample was passed through a gel filtration column (Superdex 200 column, Amersham BioSciences, Smart System).

ined, whereas oligomeric Aip2p/Dld2p bound to no substrates in the presence of ADP or with no nucleotides (data not shown). These data indicated that substrate-binding activity of oligomeric Aip2p/Dld2p requires ATP.

Gel filtration chromatography was then used to examine the oligomeric Aip2p/Dld2p–substrate interaction. Following incubation of luciferase with oligomeric Aip2p/Dld2p in the absence of ATP or presence of ADP, no oligomeric Aip2p/Dld2p–luciferase complex formation was observed, with both proteins being eluted separately (Fig. 1B, (+) ADP). In contrast, following incubation of both proteins in the presence of ATP or AMP-PNP, luciferase and oligomeric Aip2p/Dld2p eluted in fractions three and four as a complex (Fig. 1B, (+) ATP, and (+) AMP-PNP). Therefore, ATP and AMP-PNP induced the binding of oligomeric Aip2p/Dld2p to luciferase. This trend was also observed when ppαF and HMM were used as substrates (data not shown), indicating that substrate recognition is dependent on the binding of ATP to oligomeric Aip2p/Dld2p but not on ATP hydrolysis. In accordance with the result that the monomeric Aip2p/Dld2p with a C-terminal coiled-coil region-truncation failed to exhibit the conformation modifying activity [4], the coiled-coil region-truncated monomeric Aip2p/Dld2p exhibited no interaction with luciferase ((+) ATP/monomeric).

Oligomeric Aip2p/Dld2p has no obvious substrate specificity for its robust ATP-dependent protein conformation modifying activity in vitro

Oligomeric Aip2p/Dld2p increased the trypsin susceptibility of the substrate other than F-actin (ppαF, Fig. 2A, lanes 1, 2, and 4) in the presence of ATP. In the absence of ATP, however, the substrate was protected from trypsin digestion just as in the control (lanes 1 and 3), suggesting that this protein conformation modifying activity is ATP-dependent. Interestingly, further investigation revealed that the oligomeric Aip2p/Dld2p modified the conformation of actin, DNase I, the mature form of invertase, proαF, and mitochondrial SOD, as determined by the trypsin susceptibility assay (Fig. 2B). Thus, no obvious specific substrates have been identified for the protein conformation modifying activity of oligomeric Aip2p/Dld2p in vitro. Oligomeric Aip2p/Dld2p itself does not possess protease activity (Fig. 2C).

Use of the non-hydrolyzable ATP analog AMP-PNP yielded similar results to those observed with ATP, whereas the use of ADP failed to alter the luciferase activity (Fig. 2D), which is frequently used to analyze chaperone-mediated unfolding reactions as a properly folded protein substrate [12]. In accordance with our previous observation on the F-actin conformation modifying activity [4], these data further confirmed that ATP-binding rather than ATP hydrolysis is required for the protein conformation modifying reaction with other protein substrates, too.

In addition to the aforementioned indirect biochemical analyses suggesting that oligomeric Aip2p/Dld2p possesses protein conformation modifying activity, more direct evidence of this activity was sought through the use of low angle rotary shadowing [13]. Rabbit skeletal muscle HMM has a characteristic structure consisting of two globular heads and one tail (Fig. 3A, HMM). Following incubation with oligomeric Aip2p/Dld2p in the presence of 1 mM ATP, HMM heads were "unfold-

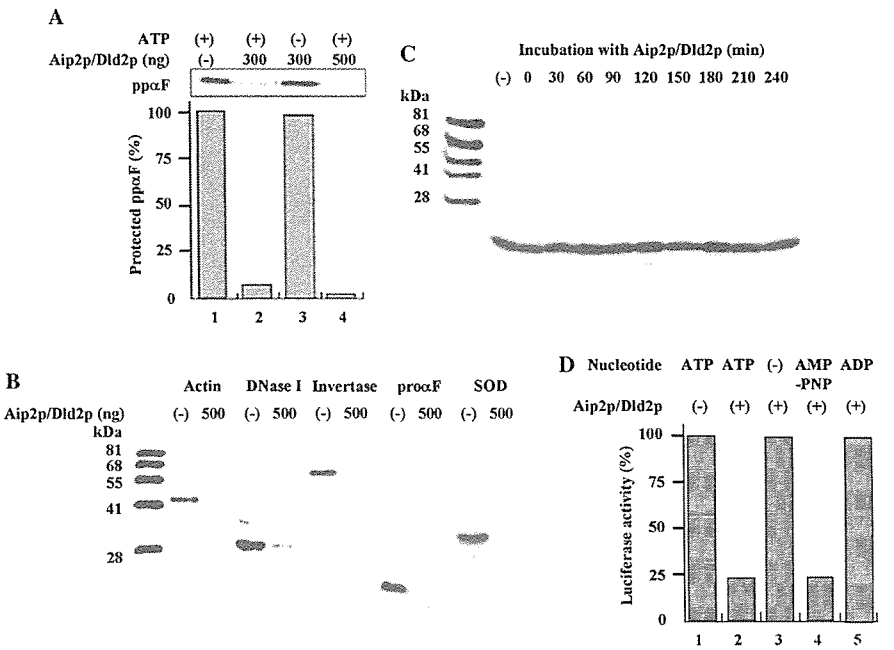

Fig. 2. Oligomeric Aip2p/Dld2p modifies the conformation of properly folded substrates in an ATP-dependent manner in vitro. (A) In the presence of ATP, Aip2p/Dld2p increases the protease susceptibility of ppαF (lanes 2 and 4). In the absence of ATP, no activity is observed (lane 3) and ppαF is resistant to trypsin digestion just as in the control (lane 1). (B) Trypsin susceptibility assay was further performed with protein substrates including actin (molecular weight = 41.8 kDa), DNase I (30 kDa), the mature form of recombinant invertase (60.6 kDa), proαF (13 kDa), and mitochondrial SOD (32.5 kDa). (C) Oligomeric Aip2p/Dld2p itself does not possess protease activity. Two hundred nanogram of ppαF was incubated with 500 ng of oligomeric Aip2p/Dld2p in the presence of 1 mM ATP for 0–240 min at 30 °C, and the signals were examined by Western blotting with anti-α-factor antibody. (D) The protein conformation modifying activity depends on ATP-binding. The firefly luciferase (300 ng) and oligomeric Aip2p/Dld2p (300 ng) were pre-incubated (final volume of 200 μl) with 1 mM ATP (lane 2), 1 mM ATP with excess amounts (10 mM) of AMP-PNP (lane 4), 1 mM ADP (lane 5) or without nucleotide (lane 3) in buffer A (see Materials and methods) for 15 min at 30 °C. The activity was assayed using the PicaGene luciferase assay kit (Wako Pure Chemicals) in a final volume of 1.2 ml, and the luciferin emission was determined using a luminometer (Stratec Biomedical Systems).

ed" and adopted an extended globular structure, while the helical tail became longer and thinner (Fig. 3A, Aip2p/Dld2p-HMM). Trypsin susceptibility of HMM also increased after the incubation with oligomeric Aip2p/Dld2p (Fig. 3A).

Surprisingly, even when pathogenic polypeptides such as the rPrP in β-sheet form, α-synuclein or amyloid β (1–42) peptide were tested as substrates in the trypsin susceptibility assay, it was found that trypsin susceptibility increased in the presence of oligomeric Aip2p/Dld2p. Although these pathogenic highly aggregated polypeptides (Fig. 3B) were resistant to 2.5 μg ml^{-1} trypsin, digestion was significant in the presence of only 200 ng ml^{-1} trypsin following incubation with oligomeric Aip2p/Dld2p (Fig. 3B).

Protein conformation modifying activity depends on the growth stage

In order to compare the protein conformation modifying activity in different cell cycles, hexahistidine-tagged oligomeric Aip2p/Dld2p was partially purified from synchronized cells during both log and stationary phases using Ni–NTA–agarose chromatography. The hexahistidine-tagged oligomeric Aip2p/Dld2p was then assayed for its protein conformation modifying activity using F-actin as a substrate. The activity of oligomeric Aip2p/Dld2p purified from log phase cells was almost fivefold greater than that measured in stationary phase cells (Fig. 4). Western blots using anti-Aip2p/Dld2p revealed that Aip2p/Dld2p expression was approximately equivalent in these two phases (Fig. 4), suggesting that the protein conformation modifying activity of oligomeric Aip2p/Dld2p varies with the cell growth stage.

Discussion

The oligomeric Aip2p/Dld2p targeted both properly folded and pathogenic highly aggregated proteins, and exhibited a robust protein conformation modifying activity in vitro. It disrupted the tertiary structure of a variety of properly and stably folded substrate proteins such as the native form of luciferase, actin, HMM, mitochondrial SOD, MDH, and DNase I, as determined in

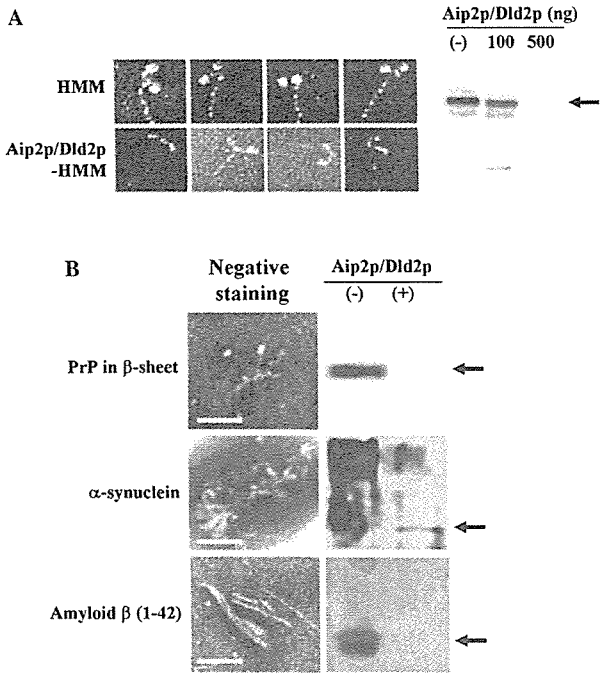

Fig. 3. Oligomeric Aip2p/Dld2p displays broad substrate specificity in vitro. (A) Heavy meromyosin (HMM) is unfolded by oligomeric Aip2p/Dld2p. One hundred microgram per milliliter of HMM was incubated with or without oligomeric Aip2p/Dld2p (100 μg ml^{-1}) in buffer A containing 1 mM ATP as described in Materials and methods. Following incubation, each mixture was subjected to low angle shadowing electron microscopy. Scale bar is 50 nm. Right panel represents the increased trypsin susceptibility of oligomeric Aip2p/Dld2p-treated HMM (100 and 500 ng). HMM was immunostained with anti-HMM polyclonal antibody. (B) Trypsin susceptibility of oligomeric Aip2p/Dld2p-treated pathogenic highly aggregated proteins is dramatically increased. Recombinant prion protein (PrP) in β-sheet form (20 μg), α-synuclein (20 μg), and amyloid β (1–42) peptide (60 μg) were used as specimens for negative staining (left panels). PrP in β-sheet form (300 ng), α-synuclein (200 ng) and amyloid β (1–42) peptide (400 ng) were used for the trypsin susceptibility assay (right panels). PrP and α-synuclein were immunostained with anti-PrP polyclonal antibody K1 (1:200) and anti-α-synuclein antibody, respectively. Amyloid β (1–42) peptide was silver stained according to the manufacturer's instruction (Wako Chemicals). Scale bars are 100 nm.

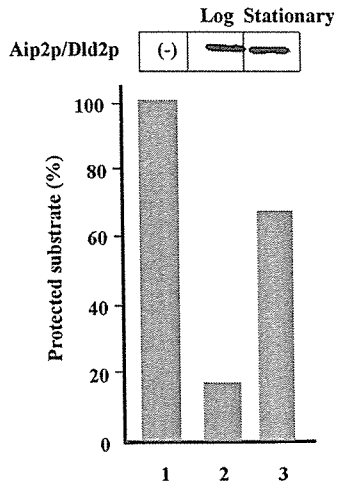

Fig. 4. Aip2p/Dld2p modifies the conformation of F-actin in vivo in a cell cycle-dependent manner. Analysis of protein conformation modifying activity of Aip2p/Dld2p in stationary and log phase yeast cells. Synchronized yeast cells constitutively expressing C-terminally hexahistidine-tagged Aip2p/Dld2p were grown to OD_{600} of 0.5 (log phase, lane 2) or 11 (stationary phase, lane 3) and oligomeric Aip2p/Dld2p was purified from 10 mg each of total yeast cells according to the procedure described in Materials and methods. Protected actin band was detected according to the procedure of trypsin susceptibility assay. A thousandth of purified Aip2p/Dld2p at log or stationary phases was detected by Western blot analysis with anti-Aip2p/Dld2p antibody.

vitro. Both the substrate-binding and protein conformation modifying activities are regulated by the binding of ATP to Aip2p/Dld2p, but not by ATP hydrolysis.

This represents a distinct profile as reflected in known Group I and II chaperonins, which do not target the properly folded proteins [14–17]. In terms of the recognition of native (properly folded) proteins, the folding of native tubulin involves at least seven different chaperone proteins [18], while the structure of the yeast homolog of cofactor A, Rbl2p, is a dimer with largely hydrophilic surfaces, reflecting the fact that it interacts with quasi-native, and not unfolded, β-tubulin. In turn, these chaperone proteins do not recognize misfolded proteins. It is worth noting that the robust protein conformation modifying activity of oligomeric Aip2p/Dld2p modulated the conformation of several pathogenic, highly aggregated proteins such as PrP in β-sheet form associated with prion disease [19], α-synuclein associated with Parkinson's disease [20], and amyloid β (1–42) peptide associated with Alzheimer's disease [21].

As an example of the three-dimensional image of proteins with increased trypsin susceptibility, we directly visualized the "unfolded" structure of substrate protein (HMM) by oligomeric Aip2p/Dld2p with the low angle rotary shadowing electron microscopy. Based on our previous notion that the oligomeric Aip2p/Dld2p exhibits a grapple-like structure of 10–12 subunits with an ATP-dependent opening [4], we are tempted to speculate that substrate proteins probably enter the cavity of oligomeric Aip2p/Dld2p, where they were unfolded in the presence of ATP. Thus, protein unfolding seems to contribute, at least in part, to the aberrant trypsin susceptibility by oligomeric Aip2p/Dld2p.

When the oligomeric Aip2p/Dld2p regulates some protein metabolism in vivo through its unique protein conformation modifying activity, the activity as it is can be extremely dangerous for cells, as it exhibits broad substrate specificity in vitro. Thus, this activity has to be tightly controlled under very stringent regulation such as by other co-factor/s in vivo. In fact, partially purified Aip2p/Dld2p at the log phase possessed higher protein conformation modifying activity and ATP-binding capacity than that of Aip2p/Dld2p purified at the sta-

tionary phase, suggesting the presence of cofactor/s that may provide ATP to oligomeric Aip2p/Dld2p in yeast cells, where F-actin is supposed to be a major target in vivo [5].

Finally, these data further support our previous notion that the oligomeric Aip2p/Dld2p may belong to an unusual class of molecular chaperones [4]. The oligomeric Aip2p/Dld2p represents a unique grapple-like structure in an ATP-dependent opening, and is able to recognize both properly folded and highly aggregated proteins with broad substrate specificity in vitro. Whether these data represent a new regulatory mechanism of protein conformations in vivo has yet to be determined.

Acknowledgments

We are indebted to G. Schatz, S.B. Prusiner, K. Mihara, and R.Scheckman for critical discussions and to I. Wada, N. Hoogenraad, M. Ryan, and A. Asano for helpful comments. We are also grateful to Y. Kozuka, K. Ihara, S. Yoshioka, M. Yamada, K. Watanabe, E.A. Nanri, and K. Ishibashi for technical assistance. This work was supported in part by grants from Exploratory Research for Advanced Technology (ERATO) and Core Research for Evolutional Science and Technology (CREST) of the Japan Science Technology Corporation (JST), Health and Labour Sciences Research Grants, Research on Advanced Medical Technology, nano-001, the Ministry of Health, Labour and Welfare of Japan, and the Naito Foundation.

References

[1] D.C. Amberg, E. Basart, D. Botstein, Defining protein interactions with yeast actin in vivo, Nat. Struct. Biol. 2 (1995) 28–35.
[2] A. Chelstowska, Z. Liu, Y. Jia, D. Amberg, R.A. Butow, Signalling between mitochondria and the nucleus regulates the expression of a new D-lactate dehydrogenase activity in yeast, Yeast 15 (1999) 1377–1391.
[3] M.J. Flick, S.F. Konieczny, Identification of putative mammalian D-lactate dehydrogenase enzymes, Biochem. Biophys. Res. Commun. 295 (2002) 910–916.
[4] N.S. Hachiya, Y. Sakasegawa, S.H.A. Jozuka, S. Tsukita K. Kaneko, Oligomeric Aip2p/Dld2p forms a novel grapple-like structure and has an ATP-dependent F-actin conformation modifying activity in vitro, Biochem. Biophys. Res. Commun. 320 (2004) 1271–1276.
[5] N.S. Hachiya, Y. Sakasegawa, A. Jozuka, S. Tsukita, K. Kaneko, Interaction of D-lactate dehydrogenase protein 2 (Dld2p) with F-actin: implication for an alternative function of Dld2p, Biochem. Biophys. Res. Commun. 319 (2004) 78–82.
[6] T.D. Pollard, The cytoskeleton, cellular motility and the reductionist agenda, Nature 422 (2003) 741–745.
[7] N.S. Hachiya, K. Watanabe, Y. Sakasegawa, K. Kaneko, Microtubules-associated intracellular localization of the NH(2)-terminal cellular prion protein fragment, Biochem. Biophys. Res. Commun. 313 (2004) 818–823.
[8] N.S. Hachiya, K. Watanabe, M. Yamada, Y. Sakasegawa K. Kaneko, Anterograde and retrograde intracellular trafficking of fluorescent cellular prion protein, Biochem. Biophys. Res. Commun. 315 (2004) 802–807.
[9] N. Hachiya, R. Alam, Y. Sakasegawa, M. Sakaguchi, K. Mihara, T. Omura, A mitochondrial import factor purified from rat liver cytosol is an ATP-dependent conformational modulator for precursor proteins, EMBO J. 12 (1993) 1579–1586.
[10] N. Hachiya, T. Komiya, R. Alam, J. Iwahashi, M. Sakaguchi T. Omura, K. Mihara, MSF, a novel cytoplasmic chaperone which functions in precursor targeting to mitochondria, EMBO J. 13 (1994) 5146–5154.
[11] N. Hachiya, K. Mihara, K. Suda, M. Horst, G. Schatz T. Lithgow, Reconstitution of the initial steps of mitochondrial protein import, Nature 376 (1995) 705–709.
[12] E. Nimmesgern, F.U. Hartl, ATP-dependent protein refolding activity in reticulocyte lysate. Evidence for the participation of different chaperone components, FEBS Lett. 331 (1993) 25–30.
[13] S. Tsukita, Desmocalmin: a calmodulin-binding high molecular weight protein isolated from desmosomes, J. Cell Biol. 101 (1985) 2070–2080.
[14] T. Laufen, M.P. Mayer, C. Beisel, D. Klostermeier, A. Mogk J. Reinstein, B. Bukau, Mechanism of regulation of hsp70 chaperones by DnaJ cochaperones, Proc. Natl. Acad. Sci. USA 96 (1999) 5452–5457.
[15] R. Russell, A. Wali Karzai, A.F. Mehl, R. McMacken, DnaJ dramatically stimulates ATP hydrolysis by DnaK: insight into targeting of Hsp70 proteins to polypeptide substrates, Biochemistry 38 (1999) 4165–4176.
[16] Y. Groemping, D. Klostermeier, C. Herrmann, T. Veit, R. Seidel, J. Reinstein, Regulation of ATPase and chaperone cycle of DnaK from *Thermus thermophilus* by the nucleotide exchange factor GrpE, J. Mol. Biol. 305 (2001) 1173–1183.
[17] J.P. Grimshaw, I. Jelesarov, H.J. Schonfeld, P. Christen, Reversible thermal transition in GrpE, the nucleotide exchange factor of the DnaK heat-shock system, J. Biol. Chem. 276 (2001) 6098–6104.
[18] J. Martin, Group II chaperonins as mediators of cytosolic protein folding, Curr. Protein Pept. Sci. 1 (2000) 309–324.
[19] M.P. Mayer, H. Schroder, S. Rudiger, K. Paal, T. Laufen B. Bukau, Multistep mechanism of substrate-binding determines chaperone activity of Hsp70, Nat. Struct. Biol. 7 (2000) 586–593.
[20] J.T. Greenamyre, T.G. Hastings, Biomedicine. Parkinson's-divergent causes, convergent mechanisms, Science 304 (2004) 1120–1122.
[21] J.W. Lustbader, M. Cirilli, C. Lin, H.W. Xu, K. Takuma N. Wang, C. Caspersen, X. Chen, S. Pollak, M. Chaney F. Trinchese, S. Liu, F. Gunn-Moore, L.F. Lue, D.G. Walker, P. Kuppusamy, Z.L. Zewier, O. Arancio, D. Stern, S.S. Yan H. Wu, ABAD directly links a beta to mitochondrial toxicity in Alzheimer's disease, Science 304 (2004) 448–452.

Available online at www.sciencedirect.com
SCIENCE DIRECT®
Biochemical and Biophysical Research Communications 313 (2004) 818–823
BBRC
www.elsevier.com/locate/ybbrc

Microtubules-associated intracellular localization of the NH_2-terminal cellular prion protein fragment

Naomi S. Hachiya, Kota Watanabe, Yuji Sakasegawa, and Kiyotoshi Kaneko*

Department of Cortical Function Disorders, National Institute of Neuroscience (NIN), National Center of Neurology and Psychiatry (NCNP), Tokyo 187-8502, Japan
Core Research for Evolutional Science and Technology (CREST), Japan Science and Technology Corporation, Japan

Received 25 November 2003

Abstract

By utilizing double-labeled fluorescent cellular prion protein (PrP^C), we revealed that the NH_2-terminal and COOH-terminal PrP^C fragments exhibit distinct distribution patterns in mouse neuroblastoma neuro2a (N2a) cells and HpL3-4, a hippocampal cell line established from *prnp* gene-ablated mice [Nature 400 (1999) 225]. Of note, the NH_2-terminal PrP^C fragment, which predominantly localized in the intracellular compartments, congregated in the cytosol after the treatment with a microtubule depolymerizer (nocodazole). Truncated PrP^C with the amino acid residues 1–121, 1–111, and 1–91 in mouse (Mo) PrP exhibited a proper distribution profile, whereas those with amino acid residues 1–52 and 1–33 did not. These data indicate the microtubules-associated intracellular localization of the NH_2-terminal PrP^C fragment containing at least the 1–91 amino acid residues.

Keywords: Prion protein; Microtubules; Fluorescent protein; Nocodazole; Proteolytic cleavage; Subcellular localization

Prion diseases are a group of neurodegenerative disorders including kuru, Creutzfeldt–Jakob disease (CJD), Gerstmann–Sträussler–Scheinker disease (GSS), and fatal familial insomnia (FFI) in humans, scrapie in sheep, and bovine spongiform encephalopathy (BSE) in cattle, which can be presented as sporadic, inherited, and infectious disorders [2]. The posttranslational conformational change of the cellular isoform of prion protein (PrP^C) into the scrapie isoform of prion protein (PrP^{Sc}) is the fundamental process underlying the pathogenesis of the prion disease [3,4]. After PrP^C is synthesized in the endoplasmic reticulum, it transits through the Golgi apparatus to the cell surface lipid rafts which is a subcellular compartment defined biochemically by membranes rich in cholesterol and glycosphingolipids, where it is bound by a glycophosphatidylinositol (GPI)-anchor [5,6] and then PrP^C is either metabolized or converted into PrP^{Sc} [7–9].

Several groups have already generated fluorescent PrP^C molecules, in which a green fluorescent protein (GFP) was either NH_2-terminally or COOH-terminally fused [10–13]. Of note, the copper treatment induced fluorescent PrP^C to be internalized like endogenous PrP^C, indicating that such fluorescent PrP^C could be functional [10]. Regardless of the position of the GFP inserts, fluorescent PrP^C in a GPI-anchored form was reported as being correctly targeted to the plasma membrane, where it is detected in lipid rafts [10,12]. However, there has been neither direct comparison of distribution profiles between NH_2-terminally and COOH-terminally fluorescent-tagged PrP^C.

With this background, we made fluorescent PrP constructs double-labeled at both NH_2- and COOH-termini, and then investigated the subcellular localization in mouse neuroblastoma neuro2a (N2a) cells, known to be infectable with PrP^{Sc} [14], and HpL3-4, a hippocampal cell line established from *prnp* gene-ablated mice [1]. Subsequently, we are tempted to investigate the association of the NH_2-terminal PrP^C fragment with cytoskeletal proteins such as microtubules and actin.

* Corresponding author. Fax: +81-42-346-1748.
E-mail address: kaneko@ncnp.go.jp (K. Kaneko).

0006-291X/$ - see front matter © 2003 Elsevier Inc. All rights reserved.
doi:10.1016/j.bbrc.2003.11.167

Materials and methods

Construction of fluorescent PrP and the deletion mutants. To express fluorescent PrP in mouse neuroblastoma cells, the EGFP gene was amplified by PCR from pEGFP (Clontech) using primers 5′-GACC GGTATGGTGAGCAAGGGCGAGGAGCTG-3′ and 5′-GACCG GTATGGTGAGCAAGGGCGAGGAGCTG-3′, digested with *Age*I, and inserted into the *Age*I site (between amino acid residues 34 and 35 in mouse (Mo) PrP) of pSPOX-MHM2PrP (a gift from Dr. S.B. Prusiner, University of California, San Francisco) [15] and the resulted plasmid was designated pSPOX-MHM2PrP::GFP. The series of deletion mutants were amplified by PCR from the pSPOX-MHM2PrP::GFP using 5′-CGGGATCCACCATGGCGAACCTTG GCTACTGGCTG-3′ as the forward primer and the following backward primers: 5′-CCG CTCGAGTCACTTGTACAGCTCGTCCATGCCGAGA-3′ (for amino acid residues 1–33 in Mo PrP), 5′-CCGCTCGAGTCACTGA GGTGGGTAACGGTT-3′ (1–52), 5′-CCGCTCGAGTCATCCTTG GCCCCATCCACC-3′ (1–91), 5′-CCGCTCGAGTCACATATGCTT CATGTTGGT-3′ (1–111), and 5′-CCGCTCGAGTCACACTACTG CCCCAGCTGC-3′ (1–121), digested with *Bam*HI and *Xho*I, and replaced with the *Bam*HI–*Xho*I fragment of pSPOX-MHM2PrP::GFP. The resulted plasmids were verified by direct DNA sequencing.

Antibodies, organelle markers, and drugs. Anti-PrP antibodies K1, K3, and K9 were rabbit polyclonal serum raised against the NH_2-termianl PrP peptides (amino acid residues 26–40, 76–90, and 196–210 in Mo PrP, respectively). Anti-COOH-terminal polyclonal PrP^C antibody M20 and anti-tubulin antibody DM1A were purchased from Santa Cruz Biotechnology and Sigma, respectively. A Golgi marker anti-GM130 and a marker for lipid raft anti-GM1 antibody were purchased from BD Biosciences and Calbiochem, respectively. As ER markers, ER-Tracker Blue-White DPX (Molecular Probes), Calnexin (Stressgen), BiP (BD Biosciences), and PDI (Stressgen) were purchased and used. Other organelle markers including an early endosomal marker EEA1 (BD Biosciences), a lysosomal marker LysoTracker Green (Molecular Probes), and a mitochondrial marker MitoTracker Red CHXROS (Molecular Probes) were also used for the experiments. Nocodazole was purchased from Sigma.

Cell cultures, DNA transfection, and drug treatments. Mouse neuroblastoma neuro2a (N2a) cells were obtained from American Tissue Culture Collection. A hippocampal cell line established from *prnp* gene-ablated mice (HpL3-4) was kindly provided by Dr. T. Onodera. Cells were grown and maintained at 37 °C in MEM supplemented with 10% fetal bovine serum. N2a and HpL3-4 cells were transiently transfected with each construct using a DNA transfection kit (Lipofectamin, Gibco-BRL). Western blot analyses were performed as described [15]. Nocodazole treatment (30 μM at 30 °C for 0, 30, and 180 min) was performed according to the previous report [16].

Immunofluorescent and fluorescence microscopy. For indirect immunofluorescence analysis, fluorescent PrP^C-transfected cells were rinsed with PBS with Ca^{2+} and Mg^{2+} (PBS(+)) and then fixed with 10% formalin in 70% PBS(+) at room temperature for 30 min. After four washes with PBS(−), the fixed cells were incubated with 10% FBS in PBS(−) at room temperature for 30 min. They were then incubated at room temperature for 1 h with antibodies at desired concentrations. After four washes with PBS(−), the cells were incubated with either Alexa488 (green) Fluor-conjugated anti-rabbit IgG (Molecular Probes) or Alexa594 (red) Fluor-conjugated anti-mouse IgG (Molecular Probes), diluted 1:200 in PBS, at room temperature for 1 h. The stained cells were washed four times with PBS(−) and mounted with SLOW FADE (Molecular Probes). Immunofluorescent or autofluorescent samples were imaged with Delta-Vision microscopy system (Applied Precision), out of focus light of the visualized images was removed by interactive deconvolution.

Immunoprecipitation of tubulin and PrP^C from the tubulin–PrP^C containing vesicular complex. Harvested N2a cells (13 dishes of 9 cm plate) were washed with PBS(−) twice, suspended in PEM buffer (100 mM Pipes, 2 mM EDTA, and 1 mM $MgCl_2$) containing protease inhibitors (5 μM each of leupeptin, pepstatin, aprotinin, antipain, and 1 mM PMSF), and homogenized 30 times at 4 °C. The homogenates were centrifuged at 3000*g* for 3 min followed by 100,000*g* at 4 °C for 30 min and then the supernatant was recovered. To stabilize tubulin, the supernatant was treated with taxol (20 μM) with 1 mM GTP at 37 °C for 20 min and kept on ice for 10 min. Monoclonal anti-tubulin antibody DM1A was adsorbed to protein A–cellurofine in PBS at 4 °C for 5 h and then used for the immunoprecipitation. PrP^C signals were detected by Western blotting with either K1 or K9 from the immunoprecipitated complex. Polyclonal K1 and K9 are suitable for Western blotting (data not shown).

Results

Subcellular localization of fluorescent PrP^C

The subcellular localization of fluorescent PrP^C was investigated by utilizing double-labeled PrP^C, GFP–PrP–DsRed, and vice versa in N2a cells (Fig. 1A). We detected a NH_2-terminal PrP^C fragment predominantly in intracellular compartments as a dot-like distribution pattern, a COOH-terminal PrP^C fragment mostly at the cell surface, and PrP^C in full length intracellularly (Fig. 1B). These results were in accordance with the behavior of endogenous PrP^C immunostained with anti-PrP polyclonal antibodies K3 against the NH_2-terminal residues 76–90 in Mo PrP (Fig. 1C, left panel), and M20 against the COOH-terminal residues in Mo PrP (Fig. 1C, right panel) and thus, excluding the possibility of an artificial distribution of fluorescent PrP^C by fusing the fluorescent proteins.

While a large proportion of intracellular PrP^C was co-localized with a Golgi marker (anti-GM130) (data not shown), signals on plasma membranes were co-localized with a marker for lipid rafts (anti-GM1) (data not shown). These results are consistent with the previous observations [11–13,17]. However, under our culture conditions with N2a and HpL3-4 cells, we were unable to demonstrate co-localization of the intracellular NH_2-terminal PrP^C fragment in a dot-like distribution pattern with known organelle markers such as ER (ER-Tracker Blue-White DPX, Calnexin, BiP, PDI), Golgi apparatus (GM130), early endosomes (EEA1), lysosomes (LysoTracker, Green), or mitochondria (MitoTracker Red CHXROS) (data not shown). Thus, such intracellular PrP^C may not reflect the distribution to any single specific organelle, but further examination has yet to be required.

Western blot analysis with polyclonal antibody K1 against the NH_2-terminal residues 26–40 in Mo PrP detected the NH_2-terminal PrP^C fragment of 17 kDa exclusively in a non-lipid raft fraction (data not shown). Further mapping of the NH_2-terminal PrP^C cleavage site was achieved by transiently expressing 3F4 (amino acids 108/111 in Mo PrP) [18] epitope-tagged MHM2 PrP^C in N2a cells. Again, 3F4 detected the NH_2-terminal PrP^C fragment in the non-lipid raft fraction (Fig. 1D). Taken together, these data indicate that such NH_2-terminal

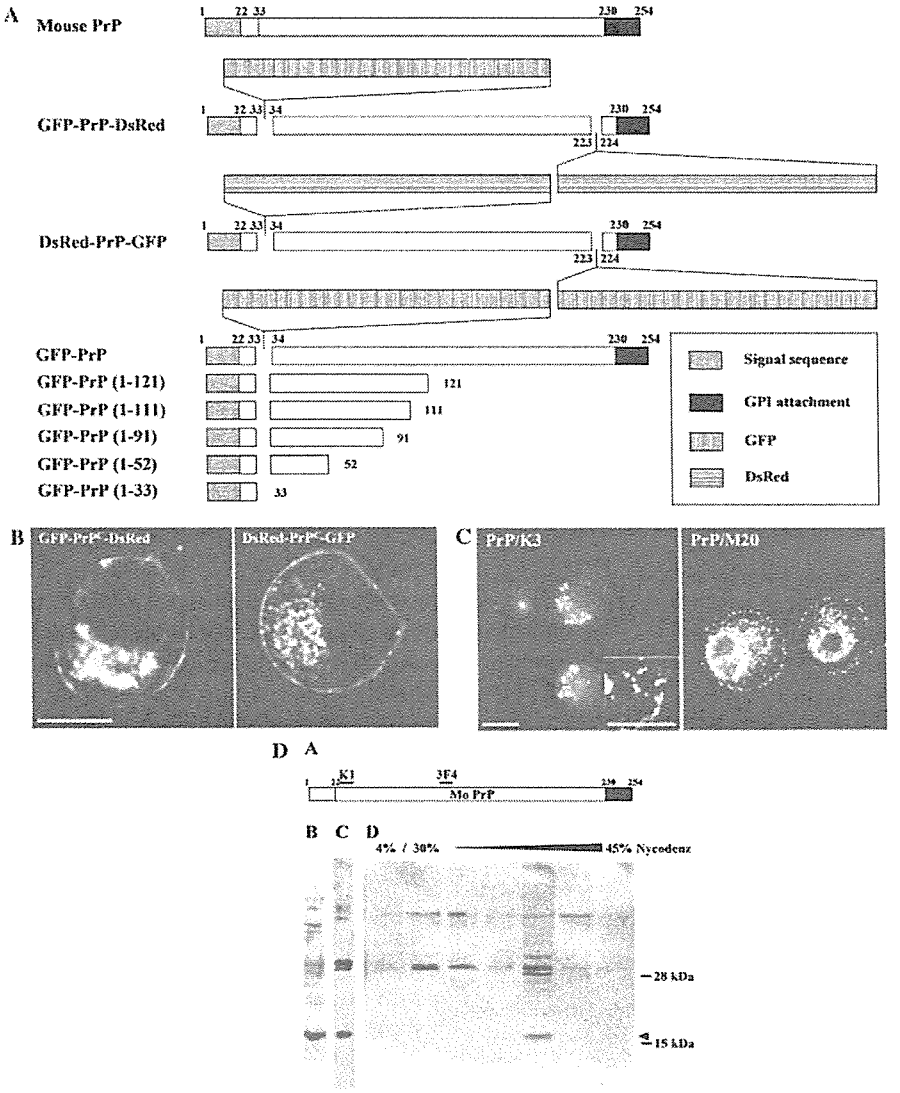

Fig. 1. Immunofluorescent analysis of fluorescent PrP^C. (A) The chimeric fluorescent PrP constructs (GFP–PrP–DsRed, DsRed–PrP–GFP, and the deletion mutant series,) used in this study. (B) Distribution patterns of GFP–PrP–DsRed (left panel): GFP–PrP^C (green) predominantly in the intracellular vesicles, PrP^C–DsRed (red) mostly at the cell surface membranes, and GFP–PrP^C–DsRed (yellow) in intracellular compartments. The DsRed–PrP–GFP (right panel) exhibits an inverted color profile indicating the same distribution patterns independent of the fluorescent conjugates. Scale bar = 8 μm. (C) Endogenous PrP^C is immunostained with anti-PrP polyclonal antibody K3 at a dilution of 1:200 (left panel) or M20 at a dilution of 1:200 (right panel). N2a cells were permeabilized with 0.1% Triton X-100. A distinct proportion of PrP^C is detected in a dot-like distribution pattern (an arrow). Scale bars = 15 μm. (D) 3F4 detects NH_2-terminal MHM2 PrP^C fragment of 17 kDa (arrow head) which was transiently transfected in N2a cells. To separate non-lipid raft fractions which contain high density, Triton X-100-insoluble intracellular membranes, we used the procedure of Naslavsky et al. [33] with slight modifications as below. Cells were lysed and resuspended in ice-cold buffer A (25 mM Hepes–KOH, pH 7.5, 5 mM EDTA, and 0.15 M NaCl) containing 1% Triton X-100, and then adjusted to 50% Nycodenz containing buffer A. Samples were centrifuged at 200,000*g* at 4 °C for 4 h by floatation in 1.5 ml of a discontinuous Nycodenz gradient (4/30/32.5/35/37.5/40/42.5/45%). After the centrifugation, samples were fractionated by 0.2 ml from the top of gradients.

PrP^C fragment contains at least residues 26–40, 76–90, and 108/111 in Mo PrP.

Microtubules-dependent intracellular localization of fluorescent PrP^C

These observations of the intracellular NH_2-terminal PrP^C fragment in a dot-like distribution pattern prompted us to further investigate its possible association with cytoskeletal proteins such as microtubules or actin. Co-immunostaining of endogenous PrP^C and microtubules by anti-PrP polyclonal antibody K3/anti-tubulin monoclonal antibody DM1A detected PrP^C along microtubules in N2a cells (Fig. 2) as well as HpL3-4 cells (data not shown). Subsequently, an immunoprecipitation assay performed with anti-tubulin antibody

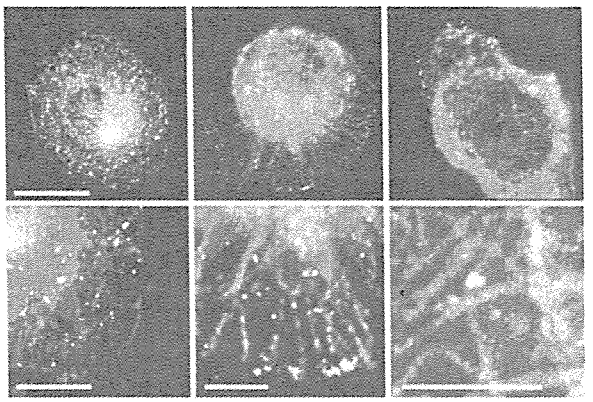

Fig. 2. Co-immunostaining of endogenous PrP^C and microtubules by anti-PrP antibody K3 (1:200, green) and anti-tubulin antibody DM1A (1:200, red) detects PrP^C along microtubules in N2a cells. Scale bar (upper panels) = 7 μm and scale bars (lower panels) = 3 μm.

(DM1A) resulted in the co-immunoprecipitation of tubulin and the NH_2-terminal PrP^C fragment of 17 kDa in N2a cells (Fig. 3A). Another polyclonal antibody K9 against the COOH-terminal residues 196–210 in Mo PrP failed to detect COOH-terminal PrP^C in the immunoprecipitated complex (Fig. 3A).

After N2a cells (Fig. 3B) were treated with 30 μM nocodazole which depolymerizes microtubules, the signals of GFP–PrP^C were congregated in a time-dependent manner. On the other hand, latrunculin A, which is widely used as an agent to sequester monomeric actin in living cells, did not affect the localization of GFP–PrP^C (data not shown). Finally, the deletion mutants (Fig. 1A) were used to map the amino acid residues responsible for the microtubules-associated localization of GFP–PrP^C. As shown in Fig. 3C, truncated constructs with the amino acid residues 1–121, 1–111, and 1–91 in Mo PrP exhibited its proper localization, whereas those with amino acid residues 1–52 and 1–33 in Mo PrP lost the dot-like distribution pattern.

Discussion

First of all, our double-labeled fluorescent PrP^C detected the NH_2-terminal and COOH-terminal PrP^C fragments with distinct subcellular distribution profiles, in which cleavage of PrP^C at around a middle region was involved [7,19,20].

Initial studies performed on the internalization of PrP^C using a chicken PrP^C have determined that endocytosis of chicken PrP is mediated by clathrin-coated pits, and the NH_2-terminal half of the chicken PrP polypeptide is essential for its endocytosis [21,22]. Recently, Nunziante et al. [23] also reported that the

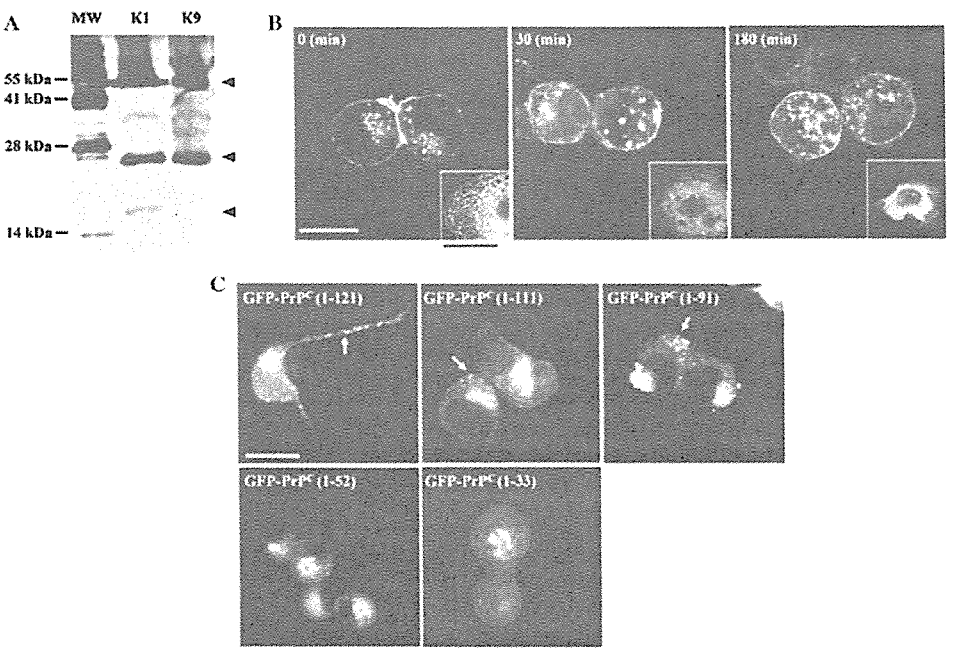

Fig. 3. The association of intracellular GFP–PrP^C with microtubules. (A) Co-immunoprecipitation of tubulin and the NH_2-terminal PrP^C fragment. Anti-tubulin antibody DM1A is used for the immunoprecipitation, and a polyclonal antibody K1 (1:500) against PrP residues 26–40 but not K9 (1:500) against residues 196–210 detects the NH_2-terminal PrP^C fragment of 17 kDa (lower arrow head) in the immunoprecipitated complex. Both K1 and K9 detect full length PrP^C (middle arrow head) and DM1A (1:2000) detects tubulin (upper arrow head). (B) After N2a cells were treated with 33 μM nocodazole and permeabilized with 0.1% Triton X-100, signals of GFP–PrP^C congregate in a time-dependent manner (0–180 min). Panels at the lower right corners represent depolymerized microtubules stained with anti-tubulin antibody DM1A (1:200). Scale bars = 15 μm. (C) The truncated GFP–PrP constructs with the amino acid residues 1–121, 1–111, and 1–91 in Mo PrP exhibit its proper localization (arrows), whereas those with 1–52 and 1–33 lose its dot-like distribution pattern. Scale bar = 15 μm.

N-proximal domain of the PrP functions as a putative targeting element and is essential for both transport to the plasma membrane and modulation of endocytosis. Along with these observations, GFP-tagged version of PrP^C was found to be properly anchored at the cell surface and its distribution pattern was similar to that of the endogenous PrP^C, with labeling at the plasma membrane and in an intracellular perinuclear compartment [10]. Further investigation concluded that PrP^C internalizes via a dynamin-dependent endocytic pathway and that the protein is targeted to the recycling endosomal compartment via Rab5-positive early endosomes and thus, traffic of GFP–PrP^C is delivered to classic endosomes after internalization [17]. Under our culture conditions, however, we could not demonstrate co-localization of the NH_2-terminal PrP^C fragment with any single specific organelle so far examined.

With this background, we have shown the microtubules-dependent intracellular localization of the NH_2-terminal PrP^C fragment in the cells. However, the question how intracellular PrP^C actually interacts with microtubules still remains to be examined. After internalized, the NH_2-terminal PrP^C fragment seems to reside inside vesicles where integral membrane proteins and linker proteins in some cases, for example, Jun kinase-interacting proteins (JIPs) [24,25], would be required for the interaction with microtubules to bridge the luminal and cytoplasmic phases across the membranes [26]. So far, we have not identified such intervening molecule/s involved in the PrP^C–microtubule interaction. Alternatively, a transmembrane form of PrP^C may be engaged in the direct interaction with the microtubules. It was suggested that a transmembrane form of PrP^C, termed C-transmembrane (^{ctm}PrP), has the COOH-terminus in the lumen with the NH_2-terminus accessible to proteases in the cytosol produced neurodegenerative changes in mice similar to those of some genetic prion diseases [27]. Such ^{ctm}PrP exposes its NH_2-terminus to the cytosol where the ^{ctm}PrP–microtubule interactions could theoretically occur, although it is less likely, as such transmembrane ^{ctm}PrP is rather pathogenic than physiologic. The fact that the truncated PrP^C with residues 1–91 cannot form ^{ctm}PrP [27], but still exhibits the microtubules-associated intracellular localization, also does not support the notion. Interestingly, these residues 1–91 partly overlap with an octapeptide repeat region, which is related to the copper metabolism [28–32]. Finally, it is also indispensable for identifying how many NH_2-terminal PrP^C fragments reside in each dot-like vesicle.

In summary, we demonstrated the microtubules-associated intracellular localization of NH_2-terminal PrP^C fragment at a steady state level. At the same time, a real time imaging analysis of fluorescent PrP^C in living cells has yet to be done toward further understanding of its mode of existence and dynamics along the microtubular network.

Acknowledgments

We greatly thank S.B. Prusiner and D.A. Harris for discussions and comments, T. Onodera for providing us the HpL3-4 cell line, M. Kawabata, E. Nannri, C. Ota, and Y. Yamaura for technical assistances. This work was supported by grants from the Core Research for Evolutional Science and Technology (CREST) of Japan Science and Technology Agency, Health and Labour Sciences Research Grants, Research on Advanced Medical Technology, nano-001, and the Ministry of Health, Labor, and Welfare of Japan.

References

[1] C. Kuwahara, A.M. Takeuchi, T. Nishimura, K. Haraguchi, A. Kubosaki, Y. Matsumoto, K. Saeki, T. Yokoyama, S. Itohara, T. Onodera, Prions prevent neuronal cell-line death, Nature 400 (1999) 225–226.
[2] S.B. Prusiner, Prions, Proc. Natl. Acad. Sci. USA 95 (1998) 13363–13383.
[3] S.B. Prusiner, D.C. Bolton, D.F. Groth, K.A. Bowman, S.P. Cochran, M.P. McKinley, Further purification and characterization of scrapie prions, Biochemistry 21 (1982) 6942–6950.
[4] S.B. Prusiner, P. Peters, K. Kaneko, A. Taraboulos, V. Lingappa, F.E. Cohen, S.J. DeArmond, Cell biology of prions, in: S.B. Prusiner (Ed.), Prion Biology and Diseases, Cold Spring Harbor, New York, 1999, pp. 349–391, Chap. 9.
[5] N. Stahl, D.R. Borchelt, K. Hsiao, S.B. Prusiner, Scrapie prion protein contains a phosphatidylinositol glycolipid, Cell 51 (1987) 229–240.
[6] B. Caughey, R.E. Race, D. Ernst, M.J. Buchmeier, B. Chesebro, Prion protein biosynthesis in scrapie-infected and uninfected neuroblastoma cells, J. Virol. 63 (1989) 175–181.
[7] A. Taraboulos, M. Scott, A. Semenov, D. Avrahami, L. Laszlo, S.B. Prusiner, Cholesterol depletion and modification of COOH-terminal targeting sequence of the prion protein inhibit formation of the scrapie isoform, J. Cell Biol. 129 (1995) 121–132.
[8] M. Vey, S. Pilkuhn, H. Wille, R. Nixon, S.J. DeArmond, E.J. Smart, R.G. Anderson, A. Taraboulos, S.B. Prusiner, Subcellular colocalization of the cellular and scrapie prion proteins in caveolae-like membranous domains, Proc. Natl. Acad. Sci. USA 93 (1996) 14945–14949.
[9] K. Kaneko, M. Vey, M. Scott, S. Pilkuhn, F.E. Cohen, S.B. Prusiner, COOH-terminal sequence of the cellular prion protein directs subcellular trafficking and controls conversion into the scrapie isoform, Proc. Natl. Acad. Sci. USA 94 (1997) 2333–2338.
[10] K.S. Lee, A.C. Magalhaes, S.M. Zanata, R.R. Brentani, V.R. Martins, M.A. Prado, Internalization of mammalian fluorescent cellular prion protein and N-terminal deletion mutants in living cells, J. Neurochem. 79 (2001) 79–87.
[11] L. Ivanova, S. Barmada, T. Kummer, D.A. Harris, Mutant prion proteins are partially retained in the endoplasmic reticulum, J. Biol. Chem. 276 (2001) 42409–42421.
[12] A. Negro, C. Ballarin, A. Bertoli, M.L. Massimino, M.C. Sorgato, The metabolism and imaging in live cells of the bovine prion protein in its native form or carrying single amino acid substitutions, Mol. Cell Neurosci. 17 (2001) 521–538.
[13] H. Lorenz, O. Windl, H.A. Kretzschmar, Cellular phenotyping of secretory and nuclear prion proteins associated with inherited prion diseases, J. Biol. Chem. 277 (2002) 8508–8516.
[14] D.A. Butler, M.A. Scott, J.M. Bockman, D.R. Borchelt, A. Taraboulos, K.K. Hsiao, D.T. Kingsbury, S.B. Prusiner, Scrapie-